國立臺灣大學管理學院財務金融學研究所

碩士論文

Institute of Finance

College of Management

National Taiwan University

Master Thesis

價差選擇權在雙資產 Merton 與 Kou 的跳躍擴散模型下之評價

Pricing Spread Options under Bivariate Merton's and Kou's Jump-Diffusion Models

張恩慈

En-Tzu Chang

指導教授: 呂育道、繆維中 博士

Advisors: Yuh-Dauh Lyuu, Wei-Chung Miao Ph.D.

中華民國 110 年 6 月

June, 2021

doi:10.6342/NTU202101125

國立臺灣大學（碩）博士學位論文
口試委員會審定書

價差選擇權在雙資產
Merton 與 Kou 的跳躍擴散模型下之評價
Pricing Spread Options under Bivariate Merton's and Kou's Jump-Diffusion Models

本論文係張恩慈君（R08723064）在國立臺灣大學財務金融學研究所完成之碩（博）士學位論文，於民國110年6月21日承下列考試委員審查通過及口試及格，特此證明

口試委員：　呂育道　繆維中　（簽名）

（指導教授）

王之彥　董夢雲

林昌碩

系主任、所長　姜堯民　（簽名）

doi:10.6342/NTU202101125

Acknowledgements

於財金所兩年的尾聲，能以這樣一篇論文作為結束，算是畫下一個完美的句點。回想起當初在決定論文題目時，身為一個財工組的學生，總覺得必須寫一篇傳統財工的題目挑戰自我，才不愧對大學讀計量財務金融並選擇財務工程組的自己，然而我卻又害怕太難的數學自己無法負荷。所幸在和繆維中教授討論過後，老師提出了一個符合我的目標又不會超出我負荷範圍的論文題目。能夠完成本篇論文，一路上我受到了許多人的幫忙及指導，在此一一感謝。

首要感謝一路上指導我的教授們，包括兩位共同指導教授呂育道老師和繆維中老師，及一路上回答我各種疑難雜症和程式指導的林昌碩老師。謝謝呂育道老師，當初願意擔任我的共同指導教授，放心讓我往自己有興趣的方向研究，並給我論文上的建議。謝謝繆維中老師擔任我的指導教授，讓我有學習的機會，也花許多心力指導我讓我踏入定價的世界。從當初修隨機過程便覺得老師很有教學及學術熱忱，和老師一起研究本篇論文的期間，更感受到老師對財務工程的熱情及研究的嚴謹度，非常感謝老師兩年來的指導，讓我收穫滿滿。謝謝林昌碩老師，即便不是我的指導教授，卻也花費許多心力，從數學式的釐清到 Matlab 程式的教學，讓我從原本一竅不通，到能自己延伸出一些結論，也謝謝老師在接近口試前，隨時回覆我的問題並花時間和我討論給我建議，讓我能如期完成論文。

感謝願意撥空擔任我們學位考試的口試委員們，謝謝王之彥老師和董夢雲老

doi:10.6342/NTU202101125

師。不僅花時間閱讀我們的論文，並在口試時給予我們修改的建議及論文的盲點。

感謝我的同學昌哲和祥恩，一起討論線上口試進行的方式，也分享彼此論文的進度，看到大家進度都差不多，我也就放心了。

最後感謝一路上不論我做什麼決定都支持我的家人，讓我能任性地做自己想做的事而無後顧之憂。也謝謝 Tim 哥，隨時被我打擾，提供我任何 Matlab 軟體、硬體上的協助，能有你們當我的後盾，真的很幸福。

doi:10.6342/NTU202101125

摘要

價差選擇權是標的為兩資產的價差的選擇權，投資人可以輕易地透過價差選擇權間接投資兩種資產，因此價差選擇權現今被廣泛應用，如利率、股票、原油及外匯市場等等。然而由於價差選擇權沒有封閉解，因此在訂價及計算希臘字母（Greeks）相對不易。並且過去文獻中多是假設資產服從幾何布朗運動，實證發現，有重大資訊宣布或極端事件發生時，資產價格會有較大的跳動，並且分配呈高峰厚尾形狀，用幾何布朗運動皆無法捕捉此特性，因此本文引用 Merton 和 Kou 的跳躍擴散模型，並延伸其隨機過程至雙資產，以針對價差選擇權訂價。除了模型的延伸，本文更是整理了過去被提出的價差選擇權近似方法及數值解，將其延伸至 Merton 和 Kou 的跳躍擴散模型下雙資產的評價，從計算精確度及效率比較，在不同模型下找到最適合的訂價引擎。

關鍵字：價差選擇權、跳躍擴散模型、二元厚尾分配、傅立葉轉換、近似解析解、高斯求積、Merton’s jump-duffusion model、Kou’s jump-duffusion model

doi:10.6342/NTU202101125

doi:10.6342/NTU202101125

Abstract

A spread option is an option written on the difference between two assets. Investors can invest in both assets or hedge through spread options thus spread options are widely applied in various markets like interest rate, stock, commodity and foreign exchange markets. However, pricing methods are still in developing and it is hard to price and calculate the Greeks since there are no closed-form solutions of spread options. Moreover, assets are assumed to follow geometric Brownian motion in most literatures in the past which are found to be unable to capture the leptokurtic feature and asymmetric fat-tailed distributions in empirical research. Therefore, in this thesis, we would review Merton's and Kou's jump-diffusion models and extend formulas to bivariate distribution. In spite of the extension of models, we also review analytical approximations and numerical integration methods and apply those methods to Merton's and Kou's jump-diffusion models. We compare all methods through accuracy and efficiency in order to find the most suitable pricing engine to price spread options under different models.

doi:10.6342/NTU202101125

Keywords: Spread option, Jump-Diffusion model, Double Exponential, Bivariate asymmetric Laplace, Fast Fourier Transform, Analytical Approximation, Gauss-Hermite Quadrature, Merton's jump-duffusion model, Kou's jump-duffusion model, double exponential jump-duffusion model

doi:10.6342/NTU202101125

Contents

Page

doi:10.6342/NTU202101125

doi:10.6342/NTU202101125

doi:10.6342/NTU202101125

doi:10.6342/NTU202101125

List of Figures

doi:10.6342/NTU202101125

doi:10.6342/NTU202101125

List of Tables

doi:10.6342/NTU202101125

doi:10.6342/NTU202101125

Denotation

BS	Black-Scholes
GBM	Geometric Browaian motion
MJD	Merton's Jump-Diffusion model
KJD	Kou's Jump-Diffusion model
BALJD	Bivariate Asymmetric Laplace Jump-Diffusion model
SO	Spread Option
BjSt	Bjerksund and Stensland
GHQ	Gauss-Hermit Quadrature
LDZ	Li, Deng and Zhou
S_i	Underlying Asset
σ_i	Volatility of one asset

doi:10.6342/NTU202101125

ρ	Correlation of both assets
ϱ	Correlation of jump size between two assets
η	Correlation of jump frequency between two assets
δ_i	Volatility of jump size
γ_i	Mean of jump size
λ_i	rate of independent Poisson process of each asset
λ_c	rate of common Poisson process
Λ_i	rate of independent Poisson process

doi:10.6342/NTU202101125

Chapter 1 Introduction

1.1 Background

A spread option is a contract written on the difference between prices of two underlying assets. Investors can investing on the spread or use spread options as hedging tools. Worth noticing, if the strike price equals to zero, spread options will be converged to exchange options. The application of spread options is widespread in energy market, interest rate derivatives and foreign exchange markets. However, the pricing and hedging methods are still underdeveloped. The reason is that there is no closed form solution for pricing spread options and closed form formulas for pricing Greeks. Besides, pricing spread options is a challenging work for we have to consider what bivariate distribution should we choose. Should we model each asset independently, model two assets simultaneously with a correlation or model the spread directly of the two assets? In this thesis, we choose the simplest way to price spread options, we assume that assets follow joint distribution with correlation on Wiener process. To capture features found in empirical research, jump-diffusion model and fat-tailed distribution are required which makes pricing spread options more difficult.

doi:10.6342/NTU202101125

1.2 Motivations

Lots of pricing methodology of spread options have been proposed recently; however, most of them are based on assumptions that assets following geometric Brownian motion (GBM). Based on background information we have mentioned, we are going to discuss jump-diffusion model with fat-tailed distributions. However, distributions departing from log-normal exacerbates the difficulty of pricing. Therefore, we are motivated to find models which have tractability and implementation and to decide desired pricing methodology under each model.

1.3 Structure

The thesis is structured as follows: In Chapter 2 we will briefly introduce four analytical approximation formulas and two numerical integration methods. We also present the results of pricing errors' analysis in the case of the Black-Scholes model and show how errors vary under selected parameters. In Chapter 3 we will extend the formulas introduced in Chapter 2 to Merton's jump-diffusion model and plot relative error between approximation and Simpson's method. Then we will discuss each jump term's contribution to spread options' price. In Chapter 4, we will further investigate how the fat-tailed distribution of jump size affects spread options' prices. In this chapter, we review Kou's jump-diffusion model whose jump size follows the bivariate asymmetric Laplace distribution; apply two-dimensional fast Fourier transform and exercise parameters' sensitivity analysis.

doi:10.6342/NTU202101125

Chapter 2 Pricing Spread Options under the Black-Scholes Model

In this chapter, we first introduce four analytical methods and two numerical integration formula for pricing spread options. Then we compare the accuracy and calculating times among these five pricing methods. We use Simpson's method with $N = 2000$ as the benchmark and to calculate differences between Simpson's method and other approximations. Finally, we draw our conclusion that GHQ and the approximation formula provided by Li, Deng and Zhou (2008) are the most suitable methods under the Black-Scholes model.

2.1 Introduction of Numerical Integration

2.1.1 Simpson's Rule

Since we are going to use Simpson's method as our benchmark, we would briefly introduce the principle and equations of Simpson's method. Simpson's rule is an integra-

doi:10.6342/NTU202101125

tion method which approximates a definite function by using quadratic functions. Below is the equation for Simpson's rule.

$$\int_a^b f(x)dx \approx \frac{\triangle x}{3}[f(x_0)+4f(x_1)+2f(x_2)+4f(x_3)+2f(x_4)+\cdots+4f(x_{n-1})+f(x_n)] \tag{2.1}$$

Simpson's rule is based on the fact that given three points, we can find the equation of a quadratic through those points. To obtain an approximation of the integral $\int_a^b f(x)dx$ using Simpson's rule, we partition the interval $[a, b]$ into an even number N of subintervals, each of width $\triangle x = \frac{b-a}{N}$. The coefficient of Simpson's equation should follow this rule: $\underbrace{1, 4, 2, 4, 2, \ldots, 4, 2, 4, 1}_{N+1}$. To strike a balance between accuracy and efficiency, we should determine how many subintervals we should choose when pricing derivatives.

In Table 2.1, we show the comparison between multiple choices of subintervals. In terms of the above subtable which shows the calculating time of each choice, we can see that under GBM, there's little difference between selected subintervals. We then take a look at the bottom subtable which shows if prices converge to a fixed number as N increases. From second row of the table, margin represents the increment of the price when we increase the number of subintervals. As demonstrated, though margins are tiny, we can still observe that the price converges when we choose $N = 2000$. Therefore, in the following discussion, we would pick $N = 2000$ as our benchmark.

doi:10.6342/NTU202101125

Apply Simpson's Rule on Spread Options

The price of a spread option under the Black-Scholes model can be written as

$$\text{ES} = e^{-rt}\text{E}\Big[(S_{1t} - S_{2t} - K)^+\Big] \tag{2.2}$$

$$= e^{-rt}\text{E}\Big[(S_{10}e^{R_{1t}} - S_{20}e^{R_{2t}} - K)^+\Big] \tag{2.3}$$

Since there are two random variables in the equation, we first fix $S_{20}e^{R_{2t}}$ as a constant so that $S_2 + K$ can be regarded as a new strike $\hat{K}$. We then replace K with $\hat{K}$ so the equation becomes the formula of a vanilla call option multiplied by the marginal pdf of R_{2t}.

$$\text{ES} = \int_{-\infty}^{\infty} e^{-rt}\text{E}\Big[\big(S_{10}e^{R_{1t}} - (S_{20}e^{x} + K)\big)^+\Big] f_{R_{2t}}(x)dx \tag{2.4}$$

$$= \int_{-\infty}^{\infty} \text{EC}(S_{10}, \hat{K}, r, \hat{q}, \hat{\sigma}, t) f_{R_{2t}}(x)dx \tag{2.5}$$

where

$$f_{R_{2t}}(x) = \frac{1}{\sigma_{R_2}\sqrt{2\pi}} e^{-\frac{1}{2}\left(\frac{x-\mu_{R_2}}{\sigma_{R_2}}\right)}$$

$$\hat{K} = S_{20}e^{x} + K$$

$$\hat{\sigma} = (1-\rho^2)\sigma_1^2$$

$$\hat{q} = q_1 - \rho\frac{\sigma_1(x-\mu_{R_2})}{\sigma_2 t} + \frac{1}{2}\rho^2\sigma_1^2$$

doi:10.6342/NTU202101125

Table 2.1: Comparison between different number of subintervals under Simpson's rule

(a) Caculating time when running for 100 times

	Simpson					
	$N = 500$	$N = 1000$	$N = 1500$	$N = 2000$	$N = 2500$	$N = 3000$
time (s)	0.008953	0.009145	0.011441	0.013708	0.018180	0.021904

(b) Spread options' prices and margins under GBM using Simpson's Rule

	$N = 500$	$N = 1000$	$N = 1500$	$N = 2000$	$N = 2500$	$N = 3000$
Price	9.997583	9.997583	9.997583	9.997583	9.997583	9.997583
Margin	-	-1.7764×10^{-15}	3.5527×10^{-15}	3.5527×10^{-15}	-1.5987×10^{-14}	1.5987×10^{-14}

2.1.2 Gauss-Hermite Quadrature

Gauss-Hermite quadrature is a kind of Gaussian quadrature for approximating the value of integrals of the following kind: [17]

$$\int_{-\infty}^{\infty} e^{-x^2} f(x)dx \approx \sum_{i=1}^{M} w_i f(x_i). \tag{2.6}$$

where M is the number of sample points used which called nodes (x_i). A quadrature formula approximates the integral of a function by the sum of its function values at a set of M points which is multiplied by aptly selected weighting coefficients. The weighting coefficient (w_i) is determined by a series of orthogonal polynomials that interpolate the function. In GHQ case, there is a standard routine to determine the abscissas (x_i) and weights (w_i).

doi:10.6342/NTU202101125

$$H_{j+1} = 2xH_j - 2jH_{j-1} \tag{2.7}$$

$$\widetilde{H}_{-1} = 0, \quad \widetilde{H}_0 = \frac{1}{\pi^{\frac{1}{4}}}, \quad \widetilde{H}_{j+1} = x\sqrt{\frac{2}{j+1}}\widetilde{H}_j - \sqrt{\frac{j}{j+1}}\widetilde{H}_{j-1} \tag{2.8}$$

$$w_i = \frac{2}{(\widetilde{H}'_j)^2} \tag{2.9}$$

$$\widetilde{H}'_j = \sqrt{2j}\widetilde{H}_{j-1} \tag{2.10}$$

As for literature of GHQ, Belle, Vanduffel and Yao presented applications of Gauss-Hermite Quadrature on different models and compared GHQ to other analytical methods in 2018 [20].

Before applying GHQ on pricing, we would like to discuss how many sample points we have to choose. From Figure 2.1, it is clear that we should use at least twenty sample points so that we can get accurate and stable results under each situations. Since we have demonstrated the number of sample points we need when pricing, in the following paragraph in this chapter, we would like to use $M = 20$ as benchmark to compare GHQ with other analytical approximations.

doi:10.6342/NTU202101125

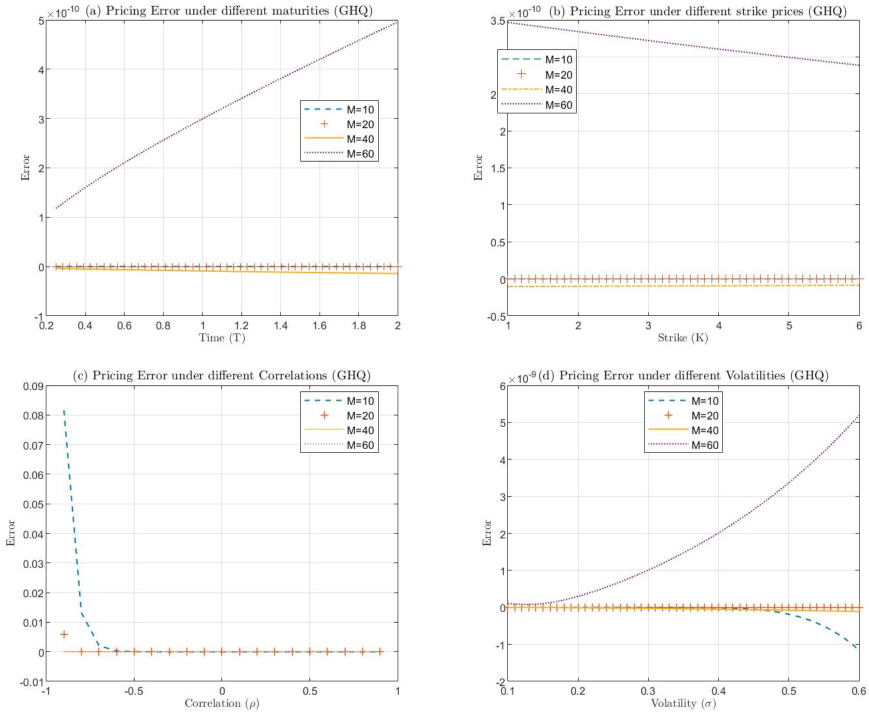

Figure 2.1: Error plots of different parameters using GHQ

2.2 Introduction to Analytical Approximations

In this section, we introduce four well-known approximation methods, which are provided by Kirk (1995) [10], Bjerksund and Stensland (2014) [4], Li, Deng and Zhou (2008) [13] and Lo (2015) [14].

In the beginning, we would like to define the equation of spread options and the stochastic differential equation of the underlying asset under Geometric Brownian motion (GBM). From equation (2.1), Π stands for the expected price of a spread option where strike price (K) is not equal to zero. Since we are pricing based on the spread between two assets, we should consider the correlation when we are calculating σ.

$$\Pi = e^{-rt}\mathrm{E}[(S_{1t} - S_{2t} - K)^{+}] \tag{2.11}$$

doi:10.6342/NTU202101125

where

$$\frac{dS_{it}}{S_{it}} = (r - q_i)dt + \sigma_i dW_{it}, \quad i = 1, 2$$

$$W_{it} \sim \mathcal{N}(0, t)$$

$$dW_1 dW_2 = \rho dt$$

Denote

$$F_i = S_{i0} e^{(r-q_i)t}$$

$$\sigma = \sqrt{\sigma_1^2 - 2b\rho\sigma_1\sigma_2 + b^2\sigma_2^2}$$

$$a = F_2 + K$$

$$b = \frac{F_2}{a}$$

doi:10.6342/NTU202101125

2.2.1 Kirk's Approximation (1995)

Kirk provided the approximation equation for spread options[10] which is extended from Margrabe's exchange option pricing formula [8]. We all know that the difference between an exchange option and a spread option is that the strike price in the Spread option is not equal to zero, which makes it no closed-form solution. Regarding of the problem, Kirk combined second asset F_2 and fixed spread K into one asset and made it a GBM if its volatility (σ_2) is a constant. Then we can apply Margrabe's formula under this situation. Below is the equation of Kirk's approximation. Π_{Kirk} denotes the present value of payoff of a spread option under Kirk's method.

$$\Pi_{\text{Kirk}} = e^{-rt}[F_1 N(d_1) - (F_2 + K)N(d_2)] \tag{2.12}$$

where N represents standard Normal cumulative probability function, and d_1, d_2 are given by

$$d_1 = \frac{\ln\left(\frac{F_1}{a}\right) + \frac{1}{2}\sigma^2 t}{\sigma\sqrt{t}},$$
$$d_2 = d_1 - \sigma\sqrt{t}$$

2.2.2 Bjerksund and Stensland's Approximation (2014)

Bjerksund and Stensland assumed that assets are log-normal and developed a feasible and flexible formula of pricing spread options [4]. There are three parts in Bjerksund and Stensland's formula (BjSt), two for each underlying asset and the rest one for strike price. And a standard normal cumulative probability follows each term.

doi:10.6342/NTU202101125

To say that the BjSt formula is quite flexible is because if $F_2 = 0$, then the formula becomes a vanilla call option formula where we can apply the Black-Scholes' equation. And if $K = 0$, then the formula becomes an exchange option formula where we can apply Margrabe's equation. Bjerksund and Stensland's formula is proved to be more precise than Kirk's formula and had a stricter lower bound than the procedure suggested by Carmona and Durrleman which needs a two-dimensional scheme. Also, Bjerksund and Stensland developed a closed-form formula for calculating Greeks of spread options which are important when considering risk management. Below is Bjerksund and Stensland's equation for pricing spread options which fits so well into the classic Black-Scholes and Margrabe's equation.

$$\Pi_{\text{BjSt}} = e^{-rt}[F_1 N(d_1) - F_2 N(d_2) - K N(d_3)] \tag{2.13}$$

where

$$\begin{aligned}
d_1 &= \frac{\ln\left(\frac{F_1}{a}\right) + \frac{1}{2}\sigma^2 t}{\sigma\sqrt{t}}, \\
d_2 &= \frac{\ln\left(\frac{F_1}{a}\right) - \frac{1}{2}(\sigma^2 - 2\rho\sigma_1\sigma_2 + (2b - b^2)\sigma_2^2)t}{\sigma\sqrt{t}}, \\
d_3 &= \frac{\ln\left(\frac{F_1}{a}\right) - \frac{1}{2}(\sigma_1^2 - b^2\sigma_2^2)t}{\sigma\sqrt{t}}
\end{aligned}$$

doi:10.6342/NTU202101125

2.2.3 Li, Deng and Zhou's Approximation (2008)

In Li, Deng and Zhou's article, they developed a faster and more accurate analytical approximation than old numerical and analytical methods [13]. To improve the accuracy and calculating efficiency, they used quadratic approximation to gain the exercise boundary thus their pricing errors are often smaller then 10^{-4}. The difference between LDZ's and other approximation methods is that they approximated each term in spread options separately. The following equation (2.14) is LDZ's approximation where F_1 means future benefit of receiving asset one, F_2 means future cost of giving up asset two when the option is expired in the money and K is the expected cost of giving up an additional monetary amount. I_i denotes one-dimensional integrals of cumulative standard normal distribution functions. Moreover, I_i has intuitive meanings, that is, I_i stands for probabilities that the spread option will expire in the money under risk-neutral and F_1, F_2 based numeraire measures. The characteristics of I_i in LDZ equation are similar to $N(d_1)$ in the Black-Scholes formula.

Finally, the improved approximation of LDZ which is based on quadratic approximation of the conditional moneyness function showed that they not only resulted in faster procedure but more accurate prices. As for detailed parameters of LDZ equation, we list them right after the equation (2.14).

$$\Pi_{\text{LDZ}} = e^{-rt}(F_1 I_1 - F_2 I_2 - K I_3) \tag{2.14}$$

where

doi:10.6342/NTU202101125

$$I_i = J_0(C_i, D_i) + J_1(C_i, D_i)\alpha + \frac{1}{2}J_2(C_i, D_i)\alpha^2$$

$$J_0(u, v) = \Phi\left(\frac{u}{\sqrt{1+v^2}}\right)$$

$$J_1(u, v) = \frac{1 + (1 + u^2)v^2}{(1 + v^2)^{\frac{2}{5}}}\phi\left(\frac{u}{\sqrt{1+v^2}}\right)$$

$$J_2(u, v) = \frac{((6 - 6u^2)v^2 + (21 - 2u^2 - u^4)v^4 + 4(3 + u^2)v^6 - 3)u}{(1 + v^2)^{\frac{11}{2}}}\phi\left(\frac{u}{\sqrt{1+v^2}}\right)$$

$$C_1 = C_3 + (D_3\rho + \sqrt{1-\rho^2})v_1 + \alpha\rho^2 v_1^2$$

$$C_2 = C_3 + D_3 v_2 + \alpha v_2^2$$

$$C_3 = \frac{\mu_1 - \ln(\beta + K)}{v_1\sqrt{1-\rho^2}}$$

$$D_1 = D_3 + 2\alpha\rho v_1$$

$$D_2 = D_3 + 2\alpha v_2$$

$$D_3 = \frac{1}{v_1\sqrt{1-\rho^2}}\left(\rho v_1 - \frac{v_2\beta}{\beta + K}\right)$$

$$\alpha = \frac{-v_2^2\beta K}{2v_1\sqrt{1-\rho^2}(\beta + K^2)}$$

$$\beta = e^{\mu_2}$$

$$\mu_i = \ln S_{i0} + \left(r - q_i - \frac{\sigma_i^2}{2}\right)t$$

$$v_i = \sigma_i\sqrt{t}$$

doi:10.6342/NTU202101125

2.2.4 Lo's Approximation (2015)

In Lo's article in 2015, Lo proposed an equation using Strang operator splitting approximation to improve Kirk's approximation without sacrificing the efficiency [14]. The aim of Lo's approximation is to wipe out the limitation of Kirk's equation which is more favorable for positive correlation. Below is Lo's approximation.

$$\Pi_{\text{Lo}} = \Pi_{\text{Kirk}} - \frac{b^2(\rho\sigma_1 - b\sigma_2)\sigma_2^3 t}{2\sigma^2} K e^{-rt} N(d_2) \times \left[d_2\Big(1 - \frac{\rho\sigma_1}{b\sigma_2}\Big) - \frac{(\rho\sigma_1 - b\sigma_2)\sigma_2\sqrt{t}}{2\sigma(S_{20} + Ke^{-rt})} K e^{-rt} \Big(d_1 d_2 + (1-\rho^2)\Big(\frac{\sigma_1}{\rho\sigma_1 - b\sigma_2}\Big)^2 \Big) \right] \tag{2.15}$$

where

$$d_1 = \frac{\ln\left(\frac{F_1}{a}\right) + \frac{1}{2}\sigma^2 t}{\sigma\sqrt{t}},$$

$$d_2 = d_1 - \sigma\sqrt{t}$$

2.3 Numerical Results

All tables and figures in this section are generated from Matlab R2020b. The basic settings of model parameters are: $S_1 = 100, S_2 = 96, r = 0.1, q_1 = 0.05, q_2 = 0.05, \sigma_1 = 0.2, \sigma_2 = 0.1, T = 1$.

doi:10.6342/NTU202101125

2.3.1 Parameters' Sensitivity

We use spread options' values obtained by Simpson's method with $N = 2000$ as exact prices and consider four of important parameters in GBM which are correlation, volatility, price of underlying assets and maturity's effect on price referred to Baeva's article in 2011 [3].

In Table 2.2, there are four subtables, each of the first three shows combination of two parameters' effect on prices. We first demonstrate combinations of strike and correlations in Table 2.2(a). In the case $K = 0$, the spread option reduces to an exchange option. In the case $K > 0$, the spread option can be seem as a call spread on price $S_1 - S_2$. In the case $K < 0$, the spread option can be seem as a put spread on the opposite price $S_2 - S_1$. Besides, we can observe that both correlation and strike have negative impacts on spread options' prices. That result is also in line with the fact that spread options on two less correlated assets tend to be more expensive.

In Table 2.2(b), we show both underlying assets' impact on spread options' prices. If we divide the table by diagonal line, interestingly, prices at upper right corner are larger than prices at the bottom left. If we fix $S_2 = 90$, we can see the prices increasing as S_1 becomes larger while prices decrease if S_1 is fixed and S_2 rises. The table sheds a light on spreads between two correlated assets have positive impact on spread options' prices.

In Table 2.2(c) comes the effect of maturity and volatility, the result is consistent with vanilla options whose Greeks, theta and vega, are positive. It is worth noting that we discuss the difference of both assets' volatility in Table 2.2(d) which shows the bigger the difference is, the higher the prices are and the greater impact of maturity on prices. As we know how parameters' affect prices, we can move on the pricing errors' analysis.

doi:10.6342/NTU202101125

Table 2.2: Parameters' sensitivity to spread options

(a) Strike & Correlation

ρ	K										
	-5	-4	-3	-2	-1	0	1	2	3	4	5
$+0.9$	9.585133	8.921378	8.286267	7.680550	7.104724	6.559048	6.043542	5.558009	5.102051	4.675087	4.276380
$+0.7$	10.494360	9.872315	9.273599	8.698582	8.147511	7.620514	7.117603	6.638677	6.183527	5.751848	5.343241
$+0.5$	11.299967	10.701929	10.124045	9.566543	9.029577	8.513225	8.017495	7.542324	7.087579	6.653065	6.238526
$+0.3$	12.026743	11.444789	10.880825	10.335007	9.807443	9.298187	8.807244	8.334570	7.880073	7.443613	7.025009
$+0.1$	12.692832	12.122618	11.568797	11.031485	10.510762	10.006669	9.519209	9.048349	8.594019	8.156116	7.734502
-0.1	13.310725	12.749567	12.203561	11.672799	11.157341	10.657221	10.172441	9.702974	9.248767	8.809737	8.385776
-0.3	13.889256	13.335359	12.795615	12.270097	11.758855	11.261915	10.779279	10.310926	9.856811	9.416869	8.991011
-0.5	14.434897	13.886991	13.352410	12.831215	12.323447	11.829127	11.348257	10.880819	10.426778	9.986077	9.558644
-0.7	14.952537	14.409684	13.879456	13.361904	12.857062	12.364950	11.885567	11.418900	10.964917	10.523572	10.094802
-0.9	15.445968	14.907453	14.380960	13.866533	13.364202	12.873982	12.395875	11.929867	11.475932	11.034031	10.604108

(b) Asset 1 & Asset 2

S_2	S_1										
	90	92	94	96	98	100	102	104	106	108	110
90	4.396164	5.280197	6.259313	7.331081	8.491846	9.736954	11.060990	12.458015	13.921789	15.445969	17.024276
92	3.731060	4.523814	5.410652	6.390562	7.461201	8.619077	9.859755	11.178077	12.568378	14.024694	15.540945
94	3.148655	3.854240	4.651614	5.541142	6.521813	7.591368	8.746468	9.982882	11.295692	12.679490	14.128571
96	2.642526	3.265949	3.977745	4.779555	5.671664	6.653065	7.721579	8.874009	10.106317	11.413807	12.791312
98	2.205898	2.752827	3.383784	4.101555	4.907629	5.802217	6.784319	7.851832	9.001694	10.230043	11.532394
100	1.831880	2.308411	2.863908	3.502131	4.225654	5.035827	5.932799	6.915575	7.982125	9.129512	10.354044
102	1.513665	1.926108	2.411946	2.975729	3.620962	4.350025	5.164143	6.063407	7.046832	8.112455	9.257458
104	1.244687	1.599381	2.021586	2.516453	3.088250	3.740250	4.474653	5.292571	6.194041	7.178090	8.242820
106	1.018746	1.321900	1.686548	2.118256	2.621883	3.201436	3.859970	4.599524	5.421103	6.324699	7.309350
108	0.830087	1.087661	1.400731	1.775107	2.216065	2.728192	3.315253	3.980102	4.724626	5.549735	6.455380
110	0.673458	0.891063	1.158317	1.481117	1.864996	2.314960	2.835338	3.429669	4.100622	4.849945	5.678461

(c) Maturity & Volatility

σ	T									
	0.1	0.2	0.3	0.4	0.5	0.6	0.7	0.8	0.9	0.10
0.9	10.595430	14.869336	18.070055	20.703049	22.965995	24.961235	26.750141	28.373085	29.858379	31.226835
0.8	9.356036	13.139270	15.978608	18.319327	20.335421	22.116894	23.717675	25.173207	26.508324	27.741269
0.7	8.116143	11.405294	13.878541	15.921338	17.684190	19.244898	20.650041	21.930211	23.106828	24.195614
0.6	6.877045	9.669648	11.773077	13.513325	15.017604	16.351629	17.554725	18.652700	19.663613	20.600712
0.5	5.640908	7.935804	9.666950	11.101292	12.342948	13.445676	14.441629	15.351899	16.191236	16.970456
0.4	4.411978	6.210168	7.568483	8.695383	9.672142	10.540707	11.326158	12.044939	12.708548	13.325408
0.3	3.200528	4.507636	5.496356	6.317659	7.030388	7.664903	8.239353	8.765632	9.252054	9.704713
0.2	2.040389	2.876266	3.509687	4.036673	4.494642	4.902896	5.272972	5.612428	5.926549	6.219204
0.1	1.111120	1.569234	1.917617	2.208310	2.461587	2.687907	2.893516	3.082510	3.257747	3.421323

(d) Difference between both Volatility

	$T=0.1$			$T=0.5$			$T=0.9$		
$\sigma_1-\sigma_2$	0	0.3	0.5	0	0.3	0.5	0	0.3	0.5
$\sigma_2=0.1$	1.111120	4.411978	6.877045	2.461587	9.672142	15.017604	3.257747	12.708548	19.663613
$\sigma_2=0.2$	2.212054	5.206454	7.587237	4.872174	11.399777	16.547167	6.424663	14.962691	21.640231
$\sigma_2=0.3$	3.312564	6.095960	8.380738	7.278111	13.329185	18.250451	9.580583	17.473736	23.833988
$\sigma_2=0.4$	4.412425	7.043997	9.235566	9.676964	15.378536	20.077737	12.719799	20.131773	26.177645
$\sigma_2=0.5$	5.511419	8.029239	10.135639	12.066387	17.499260	21.992152	15.836847	22.870685	28.620801

Note: The exact price is based on Simpson's method with $N = 2000$.
(a) $S_1 = 100$, $S_2 = 96$, $r = 0.1$, $q_1 = 0.05$, $q_2 = 0.05$, $\sigma_1 = 0.2$, $\sigma_2 = 0.1$, $T = 1$
(b) $K = 4$, $r = 0.1$, $q_1 = 0.05$, $q_2 = 0.05$, $\sigma_1 = 0.2$, $\sigma_2 = 0.1$, $T = 1$, $\rho = 0.6$
(c) $S_1 = 100$, $S_2 = 96$, $r = 0.1$, $q_1 = 0.05$, $q_2 = 0.05$, $\sigma_2 = 0.1$, $\rho = 0.6$
(d) $S_1 = 100$, $S_2 = 96$, $r = 0.1$, $q_1 = 0.05$, $q_2 = 0.05$, $\rho = 0.6$

doi:10.6342/NTU202101125

2.3.2 Pricing Errors' Analysis under Existing Approximations

In this section, we discuss the difference of relative pricing errors between four analytical methods and one integration method. We use prices calculated by Simpson's method as the benchmark and pricing errors are defined as approximation prices minus exact prices. We also analyze the efficiency of analytical methods and integration method by computing times. We first look at some simple plots to confirm which pricing method is the most stable. As we initially guess, as for accuracy, GHQ's method performs better than other analytical methods. Then we will demonstrate how many times longer GHQ needs compare to Simpson's method and LDZ's approximation by graph and show details in table. Not surprisingly, GHQ is more time-consuming than other approximation methods but less than Simpson's rule. Then we further discuss the behavioral of pricing errors within time to maturity, strike, volatility and correlation. We apply our results in the following section.

Figure 2.2 shows values of pricing errors with different values of time, strike, volatility and correlation. From Figure 2.2, we can observe that among all spread options' pricing methods, GHQ's error is relative small compared to analytical approximations under most parameters except correlation. However, pricing errors under LDZ's approximation are also tiny and are approaching zero under every selected parameter. Thus, when considering accuracy, LDZ's approximation is the best pricing method under GBM.

doi:10.6342/NTU202101125

Since parameters may have interaction with each other, we then investigate the performance of four analytical methods within two parameters. Figure 2.3 shows how pricing errors differ under four approximations with interactive influence of correlation and strike. Figure 2.3(a) shows pricing errors of Kirk's approximation. We can see that when correlation approaches 1 and -1 and when strike deviates from zero, pricing errors become larger. And Kirk's error is about 1000 times larger than other approximations. Figure 2.3(b) shows pricing errors of LDZ's approximation. Under most situations, pricing errors are approaching zero except when strike is negative and large. Figure 2.3(c) shows pricing errors of Bjerksund and Stensland. BjSt extended Kirk's formula and simulate for each term of a spread option so that pricing errors in BjSt is 1000 times smaller than Kirk's. From this graph, we can see that absolute values of pricing errors are bigger when correlation is approaching 1 and when strike is deviating from zero. Figure 2.3(d) shows pricing errors of Lo's approximation. Lo's approximation is modified based on Kirk's equation so we can see that pricing errors are close Kirk's which are around 10^{-3}. In Figure 2.3, we can still find that LDZ's method gives good results in which errors fall on 10^{-7}.

In Table 2.3 we not only display exact prices generated from Simpson' method but also shows the variation in errors generated from analytical approximations for single parameter's effect. Moreover, we compare errors when choosing a wide range of sample points under Gauss-Hermite Quadrature method. As we have shown in parameters' sensitivity table, spread options' prices are more expensive as time to maturity becomes longer, strike is smaller and when volatility is getting larger. From Table 2.3, we can also find that GHQ is the most efficient since most of pricing errors of GHQ are smaller than 10^{-10} while most pricing errors under LDZ are less than 10^{-6}.

doi:10.6342/NTU202101125

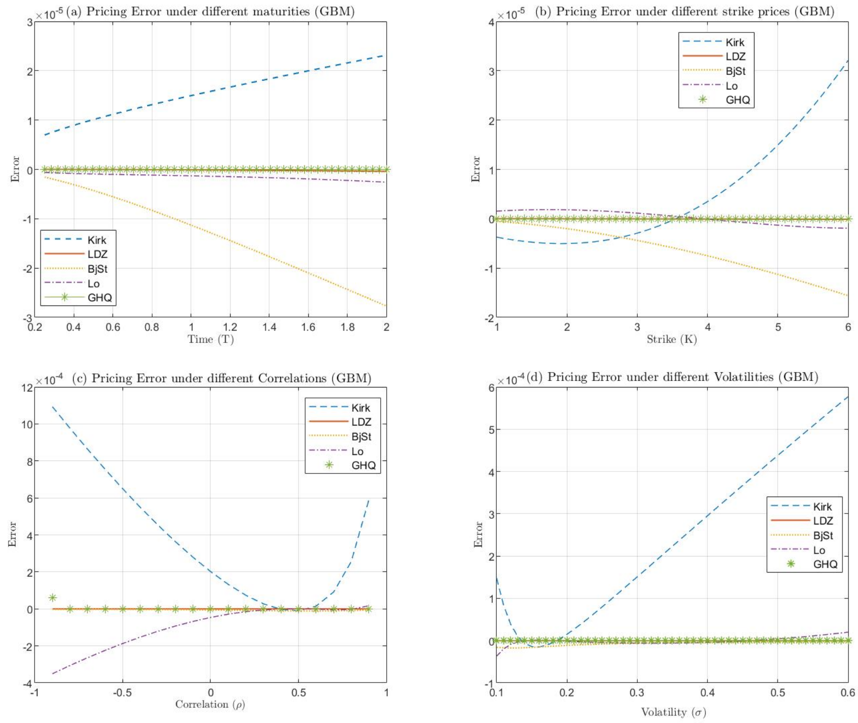

Figure 2.2: Error plots between analytical approximations and GHQ

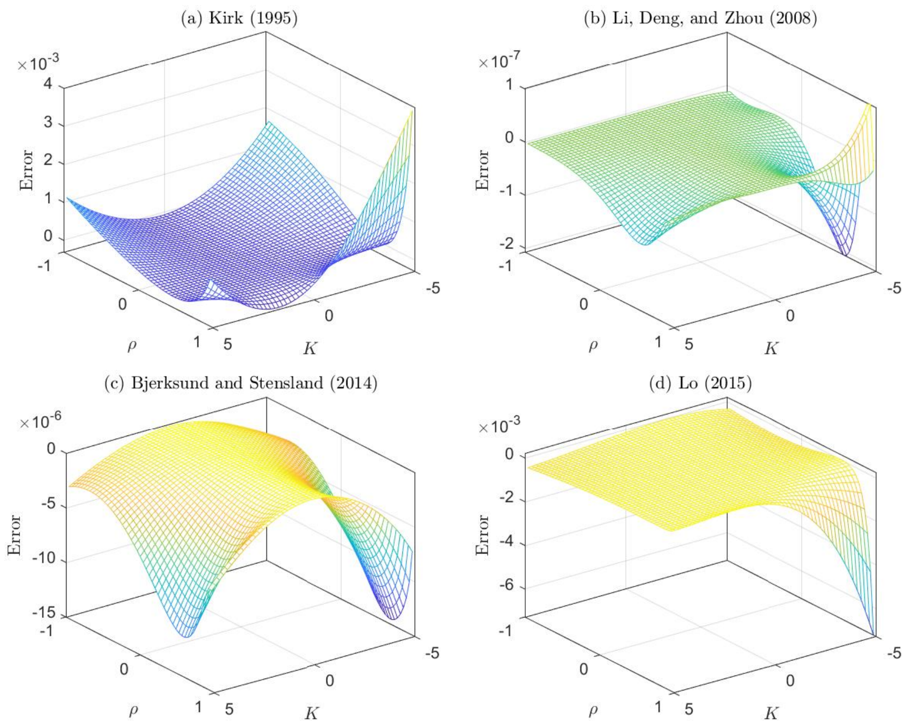

Figure 2.3: Errors' analysis of correlation and strike using analytical approximations

doi:10.6342/NTU202101125

Table 2.3 also shows pricing errors between different correlations. As we already pointed out, prices of spread options are higher when correlation is much negative. The same conclusion as we made in Table 2.3 (a) can be obtained, errors are the smallest under GHQ method which are almost less than 10^{-10}. However, what we have to be careful is, pricing errors increase when correlation is approaching -1. Therefore, if the underlying assets are strongly negative correlated, we might have to use sixty sample points to obtain accurate results.

Table 2.3: Pricing errors' analysis

(a) Maturity, Strike and Volatility

	Exact	Analytical Approx.				GHQ			
	Simpson	Kirk	LDZ	BjSt	Lo	$M=10$	$M=20$	$M=40$	$M=60$
$T=0.25$	5.176454	1.8591×10^{-4}	7.7057×10^{-7}	1.9621×10^{-4}	-3.5275×10^{-5}	-6.1391×10^{-12}	-6.1648×10^{-12}	-1.1475×10^{-12}	-1.5873×10^{-10}
$T=0.50$	7.229108	5.1650×10^{-4}	4.3726×10^{-6}	5.4447×10^{-4}	-8.2454×10^{-5}	-8.2343×10^{-12}	-8.2894×10^{-12}	-5.3291×10^{-13}	-2.3925×10^{-10}
$T=1.00$	9.997583	1.4095×10^{-3}	2.4869×10^{-5}	1.4823×10^{-3}	-1.6412×10^{-4}	-1.1408×10^{-11}	-1.1479×10^{-11}	8.9528×10^{-13}	-3.7836×10^{-10}
$T=1.50$	11.992551	2.4982×10^{-3}	6.8829×10^{-5}	2.6212×10^{-3}	-2.0679×10^{-4}	-1.4129×10^{-11}	-1.4222×10^{-11}	2.3643×10^{-12}	-5.1188×10^{-10}
$T=2.00$	13.573628	3.7106×10^{-3}	1.4177×10^{-4}	3.8845×10^{-3}	-2.0053×10^{-4}	-1.6525×10^{-11}	-1.6547×10^{-11}	4.0732×10^{-12}	-6.4747×10^{-10}
$K=10$	14.925032	4.9064×10^{-4}	4.5666×10^{-6}	4.9056×10^{-4}	-2.4771×10^{-4}	-2.4308×10^{-11}	-2.4398×10^{-11}	-9.2228×10^{-12}	1.5094×10^{-11}
$K=20$	9.997583	1.4095×10^{-3}	2.4869×10^{-5}	1.4823×10^{-3}	-1.6412×10^{-4}	-1.1408×10^{-11}	-1.1479×10^{-11}	8.9528×10^{-13}	1.2340×10^{-11}
$K=30$	6.475057	1.1494×10^{-3}	7.6586×10^{-5}	2.2259×10^{-3}	9.5561×10^{-5}	-1.1628×10^{-11}	-1.1716×10^{-11}	-1.7319×10^{-12}	9.9423×10^{-12}
$K=40$	4.087516	-9.0804×10^{-4}	1.1827×10^{-4}	2.4888×10^{-3}	-3.0791×10^{-4}	-5.9064×10^{-12}	-5.9588×10^{-12}	1.9780×10^{-12}	7.8941×10^{-12}
$K=50$	2.532732	-3.7582×10^{-3}	1.3446×10^{-4}	2.4060×10^{-3}	-1.4473×10^{-3}	-3.5105×10^{-12}	-3.0385×10^{-12}	3.1766×10^{-12}	6.1799×10^{-12}
$K=60$	1.549218	-6.1473×10^{-3}	1.4337×10^{-4}	2.1557×10^{-3}	-2.7597×10^{-3}	-1.7539×10^{-12}	-2.9849×10^{-12}	1.8188×10^{-12}	4.7713×10^{-12}
$\sigma_1=0.1$	5.366686	-4.3004×10^{-4}	2.6475×10^{-6}	9.3068×10^{-4}	3.6989×10^{-3}	-1.3835×10^{-5}	5.3381×10^{-8}	-4.1300×10^{-12}	-7.0877×10^{-13}
$\sigma_1=0.2$	6.837957	1.0206×10^{-3}	2.6242×10^{-5}	1.9069×10^{-3}	-1.3138×10^{-4}	-1.4462×10^{-11}	-1.1554×10^{-11}	-1.0981×10^{-11}	5.7909×10^{-13}
$\sigma_1=0.3$	9.997583	1.4095×10^{-3}	2.4869×10^{-5}	1.4823×10^{-3}	-1.6412×10^{-4}	-1.1410×10^{-11}	-1.1482×10^{-11}	8.9528×10^{-13}	1.2339×10^{-11}
$\sigma_1=0.4$	13.725504	-2.4555×10^{-4}	1.4844×10^{-5}	9.7164×10^{-4}	-9.1855×10^{-5}	-2.4558×10^{-11}	-2.4800×10^{-11}	1.0115×10^{-11}	3.4733×10^{-11}
$\sigma_1=0.5$	17.645785	-2.2705×10^{-3}	9.8483×10^{-6}	6.7652×10^{-4}	-1.0509×10^{-4}	-2.3626×10^{-11}	-2.4212×10^{-11}	4.0476×10^{-11}	6.4283×10^{-11}
$\sigma_1=0.6$	21.627414	-4.3428×10^{-3}	7.2316×10^{-6}	5.0471×10^{-4}	-2.1648×10^{-4}	-4.9077×10^{-11}	-4.8548×10^{-11}	5.2385×10^{-11}	1.0033×10^{-10}

(b) Correlation

	Exact	Analytical Approx.				GHQ			
ρ	(Simpson)	Kirk	LDZ	BjSt	Lo	$M=10$	$M=20$	$M=40$	$M=60$
$+0.9$	6.913100	-5.7850×10^{-3}	1.8801×10^{-6}	9.5712×10^{-4}	-9.9009×10^{-4}	-2.5924×10^{-7}	-1.2523×10^{-13}	4.3706×10^{-11}	-1.8921×10^{-9}
$+0.8$	8.072671	-1.2008×10^{-3}	1.6202×10^{-5}	1.3479×10^{-3}	-4.0353×10^{-4}	-4.0998×10^{-12}	-1.8652×10^{-13}	3.0070×10^{-11}	-1.2079×10^{-9}
$+0.7$	9.086196	7.5531×10^{-4}	2.4119×10^{-5}	1.4990×10^{-3}	-2.1321×10^{-4}	1.6520×10^{-13}	-1.1546×10^{-13}	1.9732×10^{-11}	-6.9203×10^{-10}
$+0.6$	9.997583	1.4095×10^{-3}	2.4869×10^{-5}	1.4823×10^{-4}	-1.6412×10^{-4}	1.2434×10^{-14}	-5.862×10^{-14}	1.2315×10^{-11}	-3.7838×10^{-10}
$+0.5$	10.832293	1.3233×10^{-3}	2.2221×10^{-5}	1.3793×10^{-3}	-1.3197×10^{-4}	2.8422×10^{-14}	-1.5987×10^{-14}	7.2049×10^{-12}	-2.3374×10^{-10}
$+0.4$	11.606656	7.6802×10^{-4}	1.8429×10^{-5}	1.2379×10^{-3}	-6.2577×10^{-5}	-3.5527×10^{-14}	-5.6843×10^{-14}	3.7463×10^{-12}	-2.0171×10^{-10}
$+0.3$	12.331890	-1.1112×10^{-4}	1.4569×10^{-5}	1.0848×10^{-3}	6.6121×10^{-5}	-2.4691×10^{-13}	1.5987×10^{-14}	1.6929×10^{-12}	-2.3708×10^{-10}
$+0.2$	13.016099	-1.2299×10^{-3}	1.1103×10^{-5}	9.3434×10^{-4}	2.6142×10^{-4}	7.2475×10^{-13}	-2.8422×10^{-14}	4.7784×10^{-13}	-3.1331×10^{-10}
$+0.1$	13.665365	-2.5360×10^{-3}	8.1923×10^{-6}	7.9451×10^{-4}	5.2376×10^{-4}	1.8376×10^{-10}	-7.1054×10^{-14}	-1.3500×10^{-13}	-4.1698×10^{-10}
0	14.284391	-3.9955×10^{-3}	5.8599×10^{-6}	6.6947×10^{-4}	8.5043×10^{-4}	2.7080×10^{-9}	-7.9936×10^{-14}	-3.1974×10^{-13}	-5.4232×10^{-10}
-0.1	14.876905	-5.5849×10^{-3}	4.0624×10^{-6}	5.6133×10^{-4}	1.2374×10^{-3}	1.4006×10^{-8}	-8.5265×10^{-14}	-2.8955×10^{-13}	-6.8745×10^{-10}
-0.2	15.445919	-7.2876×10^{-3}	2.7299×10^{-6}	4.7097×10^{-4}	1.6800×10^{-3}	-6.2060×10^{-8}	1.0658×10^{-14}	-1.7586×10^{-13}	-8.5296×10^{-10}
-0.3	15.993913	-9.0913×10^{-3}	1.7838×10^{-6}	3.9857×10^{-4}	2.1739×10^{-3}	-1.8189×10^{-6}	4.7091×10^{-12}	6.2172×10^{-14}	-1.0408×10^{-9}
-0.4	16.522952	-1.0987×10^{-2}	1.1456×10^{-6}	3.4392×10^{-4}	2.7145×10^{-3}	-1.9619×10^{-5}	-4.5567×10^{-11}	5.2935×10^{-13}	-1.2532×10^{-9}
-0.5	17.034784	-1.2967×10^{-2}	7.4119×10^{-7}	3.0655×10^{-4}	3.2979×10^{-3}	-1.5367×10^{-4}	-1.0628×10^{-8}	1.1475×10^{-12}	-1.4926×10^{-9}
-0.6	17.530899	-1.5025×10^{-2}	5.0281×10^{-7}	2.8588×10^{-4}	3.9201×10^{-3}	-1.0081×10^{-3}	-5.4588×10^{-7}	1.8012×10^{-12}	-1.7616×10^{-9}
-0.7	18.012582	-1.7157×10^{-2}	3.6928×10^{-7}	2.8129×10^{-4}	4.5778×10^{-3}	-5.9154×10^{-3}	-1.9267×10^{-5}	-3.9404×10^{-10}	-2.0643×10^{-9}
-0.8	18.480949	-1.9359×10^{-2}	2.8613×10^{-7}	2.9210×10^{-4}	5.2676×10^{-3}	-3.2352×10^{-2}	-5.6308×10^{-4}	-3.6380×10^{-7}	-2.7270×10^{-9}
-0.9	18.936980	-2.1627×10^{-2}	2.0524×10^{-7}	3.1768×10^{-4}	5.9867×10^{-3}	-1.6986×10^{-1}	-1.4965×10^{-2}	-2.4089×10^{-4}	-5.3408×10^{-6}

Note:
$S_1 = 100$, $S_2 = 90$, $r = 0.05$, $q_1 = 0.03$, $q_2 = 0.02$, $\sigma_2 = 0.2$

doi:10.6342/NTU202101125

2.3.3 Further Investigation of Gauss-Hermite Quadrature

As we found that GHQ is a relative better method compared to analytical approximations, we would like to further analyze GHQ's method. In Table 2.4, we show values of pricing errors under diverse situations. One thing that we should mention is that in Table 2.4, we only display pricing errors larger than 10^{-6}, for those less than 10^{-6} we replaced them with bars. The insight Of the Table 2.4 (a) is that if sample points are chosen to be forty or sixty, most errors are less than 10^{-6}. Few exceptions are when correlation is less equal to -0.8. In Table 2.4 (b), we find that under different value of volatility and maturity, most pricing errors are less than 10^{-6} except $M = 5$.

Going deep into pricing errors associated with different sample points for each strike and correlation value. Figure 2.4 displays the three-dimensional graph which we narrow down the range of correlation to $\rho = -0.8$ to $\rho = -1$. Apparently, the surfaces of pricing errors are more fluctuating. However, such phenomenon disappears when correlation is larger than 0.8. In practice, most market price of assets are positively correlated so using GHQ is still to make a choice between efficiency and accuracy.

doi:10.6342/NTU202101125

Table 2.4: Pricing errors of GHQ

(a) Correlation & Strike

ρ		$K=1$					$K=3$					$K=5$				
	M	5	10	20	40	60	5	10	20	40	60	5	10	20	40	60
0.9		−0.001128	0.000001	–	–	–	−0.001263	0.000002	–	–	–	−0.000980	–	–	–	–
0.7		–	–	–	–	–	–	–	–	–	–	–	–	–	–	–
0.5		–	–	–	–	–	–	–	–	–	–	–	–	–	–	–
0.3		–	–	–	–	–	–	–	–	–	–	–	–	–	–	–
0.1		–	–	–	–	–	–	–	–	–	–	–	–	–	–	–
−0.1		−0.000056	–	–	–	–	−0.000058	–	–	–	–	−0.000056	–	–	–	–
−0.3		−0.000960	–	–	–	–	−0.000988	–	–	–	–	−0.000949	–	–	–	–
−0.5		−0.009402	0.000041	–	–	–	−0.009642	0.000043	–	–	–	−0.009224	0.000040	–	–	–
−0.7		−0.069485	0.002138	0.000004	–	–	−0.071177	0.002254	0.000005	–	–	−0.067826	0.002044	0.000004	–	–
−0.9		−0.455152	0.086542	0.006630	0.000078	0.000001	−0.466988	0.091132	0.007397	0.000099	0.000002	−0.441932	0.081617	0.005885	0.000061	–

ρ		$K=-1$					$K=-3$					$K=-5$				
	M	5	10	20	40	60	5	10	20	40	60	5	10	20	40	60
0.9		−0.000730	–	–	–	–	−0.000282	–	–	–	–	0.000047	–	–	–	–
0.7		–	–	–	–	–	–	–	–	–	–	–	–	–	–	–
0.5		–	–	–	–	–	–	–	–	–	–	–	–	–	–	–
0.3		–	–	–	–	–	–	–	–	–	–	–	–	–	–	–
0.1		–	–	–	–	–	–	–	–	–	–	–	–	–	–	–
−0.1		−0.000048	–	–	–	–	−0.000034	–	–	–	–	−0.000013	–	–	–	–
−0.3		−0.000852	–	–	–	–	−0.000658	–	–	–	–	−0.000377	–	–	–	–
−0.5		−0.008433	0.000031	–	–	–	−0.006721	0.000014	–	–	–	−0.004324	−0.000010	–	–	–
−0.7		−0.062485	0.001665	0.000002	–	–	−0.050386	0.000865	−0.000001	–	–	−0.033899	−0.000170	−0.000005	–	–
−0.9		−0.406396	0.067886	0.003615	–	–	−0.324735	0.037720	−0.000822	−0.000091	−0.000003	−0.217856	0.000832	−0.005267	−0.000135	−0.000002

(b) Volatility & Maturity

σ_1		$T=0.15$					$T=0.3$					$T=0.45$				
	M	5	10	20	40	60	5	10	20	40	60	5	10	20	40	60
0.9		−0.000091	–	–	–	–	−0.000062	–	–	–	–	−0.000008	–	–	–	–
0.8		−0.000070	–	–	–	–	−0.000057	–	–	–	–	−0.000027	–	–	–	–
0.7		−0.000048	–	–	–	–	−0.000045	–	–	–	–	−0.000030	–	–	–	–
0.6		−0.000028	–	–	–	–	−0.000029	–	–	–	–	−0.000023	–	–	–	–
0.5		−0.000012	–	–	–	–	−0.000014	–	–	–	–	−0.000012	–	–	–	–
0.4		−0.000003	–	–	–	–	−0.000004	–	–	–	–	−0.000004	–	–	–	–
0.3		–	–	–	–	–	–	–	–	–	–	–	–	–	–	–
0.2		–	–	–	–	–	–	–	–	–	–	–	–	–	–	–
0.1		–	–	–	–	–	−0.000001	–	–	–	–	−0.000001	–	–	–	–

σ_1		$T=0.6$					$T=0.75$					$T=0.9$				
	M	5	10	20	40	60	5	10	20	40	60	5	10	20	40	60
0.9		0.000056	–	–	–	–	0.000121	–	–	–	–	0.000183	–	–	–	–
0.8		0.000012	–	–	–	–	0.000054	–	–	–	–	0.000096	–	–	–	–
0.7		−0.000010	–	–	–	–	0.000013	–	–	–	–	0.000038	–	–	–	–
0.6		−0.000015	–	–	–	–	−0.000004	–	–	–	–	0.000007	–	–	–	–
0.5		−0.000010	–	–	–	–	−0.000006	–	–	–	–	−0.000002	–	–	–	–
0.4		−0.000003	–	–	–	–	−0.000003	–	–	–	–	−0.000002	–	–	–	–
0.3		–	–	–	–	–	–	–	–	–	–	–	–	–	–	–
0.2		–	–	–	–	–	–	–	–	–	–	–	–	–	–	–
0.1		−0.000001	–	–	–	–	−0.000001	–	–	–	–	−0.000001	–	–	–	–

Note: In this table, we replace pricing errors which are less than 10^{-6} with $-$.

doi:10.6342/NTU202101125

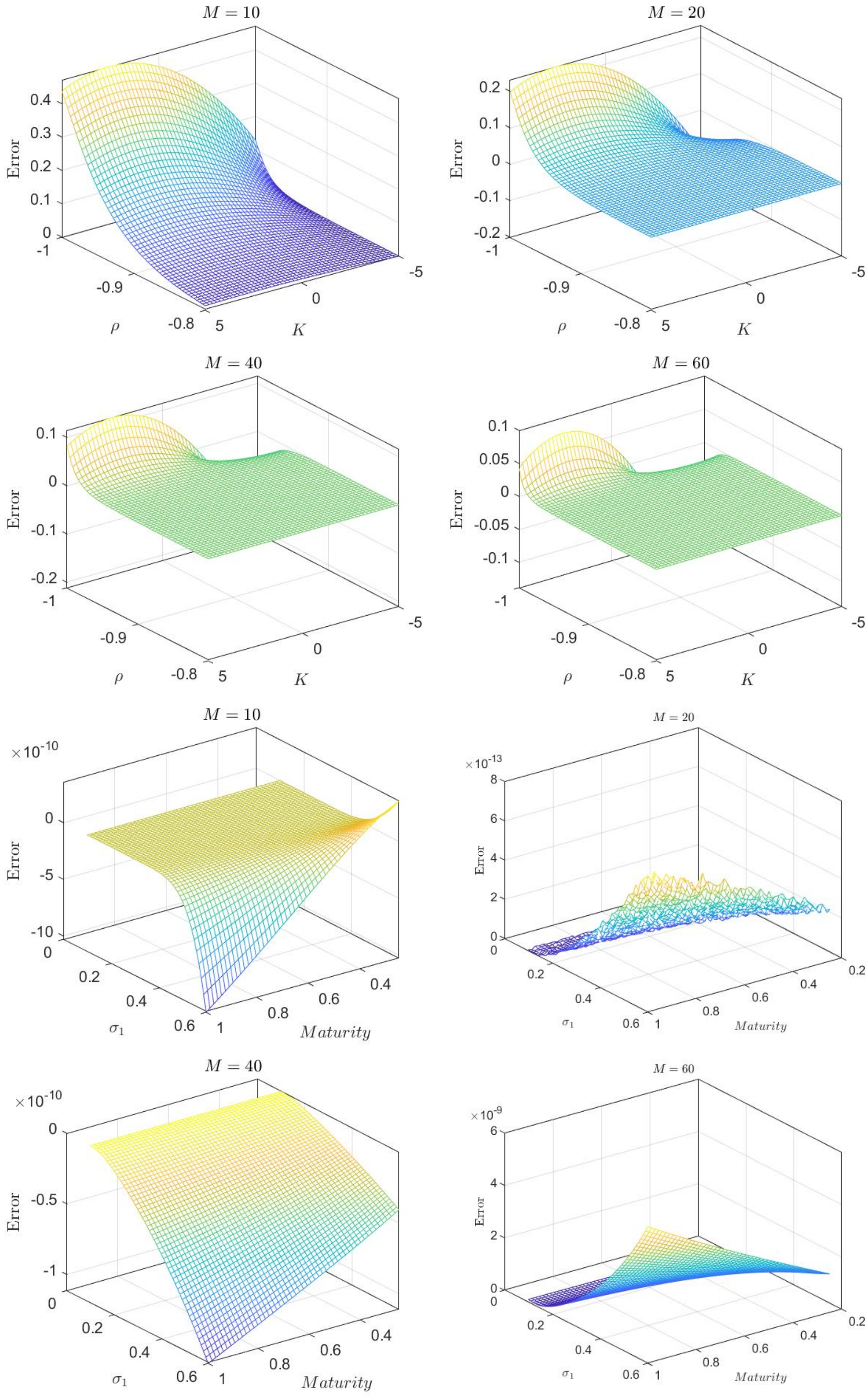

Figure 2.4: Errors' analysis within two parameters using GHQ

doi:10.6342/NTU202101125

When deciding what method should we apply on derivative pricing, calculating time is an indispensable issue that we can't ignore. Since we use Simpson's rule as benchmark and find LDZ's approximation is the best among four analytical methods we've discussed, we show figures in advance and give details in the table later. Figure 2.5 shows how much more time GHQ needs when comparing to Simpson's method and LDZ's approximation. From Figure 2.5(a), we know that GHQ is more time-consuming than Simpson's method and LDZ's method. In addition, readers are able to find out the exact numbers of calculating time of all methods we mentioned above in Table 2.5. Calculating times of analytical methods are with little difference while it takes a little longer time when using GHQ. Though GHQ seems to be more time-consuming than analytical approximations, the calculating of GHQ is not much longer than that of LDZ. Thus, from computational efficiency we can conclude that GHQ and LDZ are comparable.

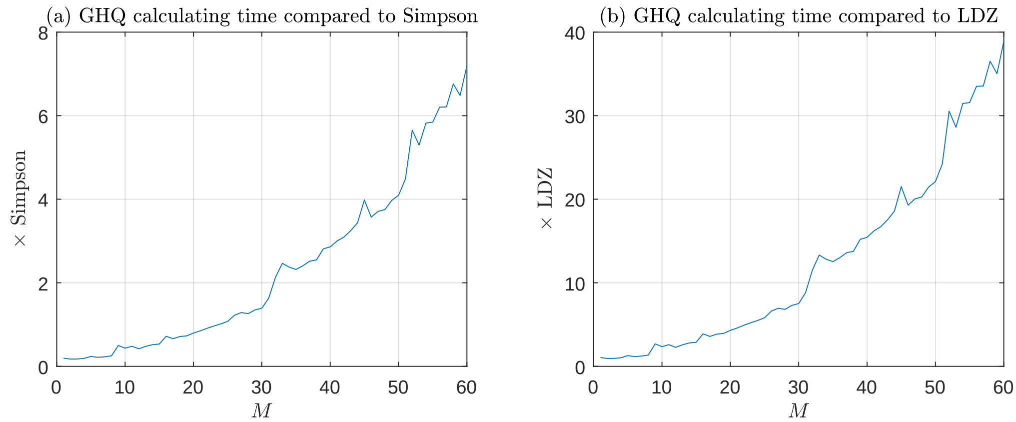

Figure 2.5: Comparison of calculating time

Table 2.5: Calculating time comparison between different pricing methods

	Calculating time when running for 100 times								
	Simpson	Kirk	Bjerksund and Stensland	Lo	Li, Deng and Zhou	GHQ			
	$N = 2000$					$M = 10$	$M = 20$	$M = 40$	$M = 60$
time (s)	0.013808	0.006680	0.009293	0.007742	0.012715	0.019074	0.018761	0.059977	0.151187

doi:10.6342/NTU202101125

2.4 Conclusions

In this chapter, we introduce existing analytical approximations and numerical integration specified in Gauss-Hermite Quadrature. We also compare the accuracy under many situations. Finally, we demonstrate the computational analysis of these methods. Given those we've investigated, we can conclude that under the simplest model GBM, LDZ's approximation and GHQ are equally matched in efficiency and accuracy. We then summarize shortcomings of the above two methods under parameters of the diffusion model in Table 2.6. In Table 2.6, we use the value of 10^{-5} as a boundary, if pricing errors are less than 10^{-5} in all situations we would tick the checkbox. In GHQ case, only when correlation is extremely negative, pricing errors are magnified to 10^{-2}. While in LDZ case, when we extend the maturity and larger the strike price, pricing errors are diverged.

Table 2.6: Comparison between GHQ and LDZ

	Pricing methods	
Parameters	GHQ	LDZ
Maturity	V	Unstable as maturity becomes longer.
Strike	V	Unstable as strike price becomes larger.
Volatility	V	V
Correlation	Unstable as correlation becomes extremely negative.	V

doi:10.6342/NTU202101125

doi:10.6342/NTU202101125

Chapter 3 Pricing Spread Options under Merton's Jump-Diffusion Model

All the literatures cited in the previous chapter assume that assets follow geometric Brownian motion which only includes diffusion process. Since spread options are often applied on energy markets, stocks or interest rate derivatives, pricing with pure diffusion process seems to be not enough and can not capture characteristics well of underlying assets. For the reasons mentioned above, we would like to extend the existing methods discussed in Chapter 2 to stochastic process with jump term. In this chapter, we review Merton's jump-diffusion model, whose jump size is assumed to follow normal distribution. Also, we extend Merton's model to spread options' formulas and derive equations of analytical approximations mentioned in previous chapter. Finally through analyzing accuracy and efficiency with jump terms, we draw the conclusion that GHQ is the most adequate pricing method under Merton's jump-diffusion model.

doi:10.6342/NTU202101125

3.1 Merton's Jump-Diffusion model

In the beginning, we would like to review Merton's jump-diffusion model. Empirical results showed that there are too many outliers for a simple Black-Scholes model especially when being in response to some announcement. Merton proposed a pricing model in 1976 to capture abnormal vibration of stock price [16]. In addition to the original Black-Schole's model, Merton added a jump component composed of lognormal jumps in stochastic process and used Poisson process to describe the dynamic of the jump term. It is assumed that the arrivals of important information are independent and identical distributed. Therefore the equation of Merton's jump-diffusion model can be written as below,

$$\frac{dS_t}{S_t} = \mu dt + \sigma dW + dJ_t \tag{3.1}$$

$$J_t = \sum_{j=1}^{N_t} (e^{Y_t} - 1) \tag{3.2}$$

$$N_t \sim \text{Pois}(\lambda t) \tag{3.3}$$

$$\ln Y_t \sim \mathcal{N}(\gamma, \delta^2) \tag{3.4}$$

doi:10.6342/NTU202101125

In Merton's jump-diffusion model, jump size $\ln Y_t$ is assumed to follow Normal distribution and jump frequency N_t is assumed to follow Poisson process. Thus, the whole jump term can be regarded as a compound Poisson process. In our case, to analyze the correlation of two assets, we divide jumps into common jumps and independent jumps where there are correlations between common jumps. Since spread options are written on the spread of two assets, jump sizes and jump frequencies should follow bivariate distribution. Thus, before presenting the equations of spread options under Merton's jump-diffusion model, we assume that readers had already understood basic knowledge of bivariate distributions. If not, readers can first read derivations of bivariate distributions in Appendix A.

3.2 Extended Formulas to the Underlying Assets under Merton's JD

With basic knowledge of bivariate distributions, we can now move on to stochastic differential equations (SDE) for each underlying assets S_{it}. Following Merton's model, S_{it} is assumed to follow the SDE below. As you can observe, the SDE adds a jump term dJ_{it} with original diffusion term and drift term. Whereas W_{it} denotes Wiener process.

$$\frac{dS_{it}}{S_{it}} = \mu_i dt + \sigma_i dW_{it} + dJ_{it}, \quad i = 1, 2 \tag{3.5}$$

doi:10.6342/NTU202101125

where

$$W_{it} \sim \text{N}(0,t), \quad dW_1 dW_2 = \rho dt$$

$$J_{it} = \sum_{j=1}^{N_{it}} (e^{Y_{ij}} - 1) + \sum_{j=1}^{N_{ct}} (e^{Y_{ij}^c} - 1), \quad i = 1,2$$

$$N_{it} \sim \text{Pois}(\lambda_i t), \quad N_{ct} \sim \text{Pois}(\lambda_c t)$$

Given the initial value, S_{i0}, the SDE can be solved to obtain

$$S_{it} = S_{i0} \exp\left(\left(\mu_i - \frac{\sigma_i^2}{2}\right)t + \sigma_i W_{it} + \sum_{j=1}^{N_{it}} \ln Y_{ij} + \sum_{j=1}^{N_{ct}} \ln Y_{ij}^c\right) \tag{3.6}$$

Denote

$$\nu_{it} = \left(\mu_i - \frac{\sigma_i^2}{2} t\right), \quad D_{it} = \nu_{it} + \sigma_i W_{it}, \quad X_{it} = \sum_{j=1}^{N_{it}} \ln Y_{ij} + \sum_{j=1}^{N_{ct}} \ln Y_{ij}^c$$

Where diffusion terms D_{it} of underlying assets follow bivariate Normal distribution as follows,

$$(D_{1t}, D_{2t}) \sim \text{BN}(\nu_1 t, \nu_2 t, \sigma_1^2 t, \sigma_2^2 t, \rho)$$

And each jump size $\ln Y_{it}$ of the jump term follows Normal distribution. While in the case of spread options, we assume that jump sizes follow bivariate Normal distribution.

$$\ln Y_{ij} \sim \mathcal{N}(\gamma_i, \delta_i^2)$$

$$(\ln Y_{1j}^c, \ln Y_{2j}^c) \sim \text{BN}(\gamma_1, \gamma_2, \delta_1^2, \delta_2^2, \varrho)$$

doi:10.6342/NTU202101125

Following the assumptions in Merton's model, we use the Poisson process to describe the dynamics of jump frequency. We then separate jumps M_{it} to the common jump N_{ct} and the independent jump N_{it} so that we could build correlations via common jumps. Equations are as follows.

Denote $M_{it} = N_{it} + N_{ct}$ and $\Lambda_i = \lambda_i + \lambda_c$

$$(M_{1t}, M_{2t}) \sim \mathrm{BP}(\Lambda_1, \Lambda_2, \eta)$$

Since we describe the jump size and the jump frequency with the bivariate Normal distribution and the bivariate Poisson process respectively, the jump term X_{it} can be regarded as a compound Poisson process. Conditioned on $M_{it} = m_i$, we can derive the distribution of jump terms.

$$(X_{1t}, X_{2t} | N_t = \big(n_1, n_2, n_c)\big) \sim \mathrm{BN}(m_1\gamma_1, m_2\gamma_2, m_1\delta_1^2, m_2\delta_2^2, \varphi)$$

where correlation of jump process can be calculated as

$$\begin{aligned}
\varphi = \mathrm{Corr}(X_{1t}^{(m_1)}, X_{2t}^{(m_2)}) &= \frac{\mathrm{Cov}\Big(\sum_{j=1}^{n_c} \ln Y_{1j}^c, \sum_{j=1}^{n_c} \ln Y_{2j}^c\Big)}{\sqrt{\mathrm{Var}\Big(X_{1t}^{(m_1)}\Big)\mathrm{Var}\Big(X_{2t}^{(m_2)}\Big)}} \\
&= \frac{\sum_{j=1}^{n_c} \mathrm{Cov}\big(\ln Y_{1j}^c, \ln Y_{2j}^c\big)}{\sqrt{\Big(\mathrm{Var}\Big(\sum_{j=1}^{n_1} \ln Y_{1j}\Big) + \mathrm{Var}\Big(\sum_{j=1}^{n_c} \ln Y_{1j}^c\Big)\Big)}\sqrt{\Big(\mathrm{Var}\Big(\sum_{j=1}^{n_2} \ln Y_{2j}\Big) + \mathrm{Var}\Big(\sum_{j=1}^{n_c} \ln Y_{2j}^c\Big)\Big)}} \\
&= \frac{n_c\varrho}{\sqrt{m_1 m_2}}
\end{aligned}$$

doi:10.6342/NTU202101125

After deriving stochastic process, we can obtain return distribution of underlying assets. With return distribution, prices of underlying assets on expiry date can be simulated so that we can calculate the theoretical spread options' prices. Follows are the formulas of return distribution.

$$R_{it} = \left(\mu_i - \frac{\sigma_i^2}{2}\right)t + \sigma_i W_{it} + \sum_{j=1}^{N_{it}} \ln Y_{ij} + \sum_{j=1}^{N_{ct}} \ln Y_{ij}^c = D_{it} + X_{it} \tag{3.7}$$

$$\Big(R_{1t}, R_{2t} | N_t = (n_1, n_2, n_c)\Big) \sim \text{BN}\Big(\nu_{1t} + m_1\gamma_1, \nu_{2t} + m_2\gamma_2, \sigma_1^2 t + m_1\delta_1^2, \sigma_2^2 t + m_2\delta_2^2, \phi\Big) \tag{3.8}$$

where

$$\begin{aligned}
\phi &= \text{Corr}\Big(R_{1t}^{(m_1)}, R_{2t}^{(m_2)}\Big) \\
&= \frac{\text{Cov}\Big(D_{1t}, D_{2t}\Big) + \text{Cov}\Big(X_{1t}^{(m_1)}, X_{2t}^{(m_2)}\Big)}{\sqrt{\text{Var}\Big(R_{1t}^{(m_1)}\Big)\text{Var}\Big(R_{2t}^{(m_2)}\Big)}} \\
&= \frac{\sigma_1\sigma_2 t\rho + n_c\delta_1\delta_2\varrho}{\sqrt{\sigma_1^2 t + m_1\delta_1^2}\sqrt{\sigma_2^2 t + m_2\delta_2^2}}
\end{aligned}$$

under the Martingale condition, μ_i should be

$$\begin{aligned}
\mu_i &= (r - q_i) - \frac{\ln\left(\text{E}^{\mathbb{Q}}[e^{X_{it}}]\right)}{t} \\
&= r - q_i - \Lambda_i k_i
\end{aligned}$$

where

doi:10.6342/NTU202101125

$$k_i = \mathrm{E}^{\mathbb{Q}}\left[e^{\ln Y_i}\right] - 1 = e^{\gamma_i + \frac{1}{2}\delta_i^2} - 1$$

3.3 Spread Option Pricing Formulas

Let's get into the topic after deriving dynamics of underlying assets. When pricing spread options, it is complicated to integrate the formula composed of two random variables. To make it simple, we integrate the formula conditioned on S_2 equals to a constant. Therefore the formula can be regarded as the one for a vanilla option. Formulas of vanilla options can be found in Appendix B. Following formulas show that how we reconstruct return distributions under the Black-Scholes model to the ones under jump-diffusion model.

We first review how price of a spread option under the Black-Scholes model can be written

$$\mathrm{ES}_{\mathrm{BS}} = e^{-rt} e\left[(S_{1t} - S_{2t} - K)^+\right] = e^{-rt} e\left[(S_{10} e^{R_{1t_{\mathrm{BS}}}} - S_{2t} e^{R_{2t_{\mathrm{BS}}}} - K)^+\right] \tag{3.9}$$

where

$$R_{it_{\mathrm{BS}}} = \left(r - q_i - \frac{1}{2}\sigma_1^2\right)t + \sigma_i W_{it}$$
$$(R_{1t_{\mathrm{BS}}}, R_{2t_{\mathrm{BS}}}) \sim \mathrm{BN}\left(\left(r - q_1 - \frac{1}{2}\sigma_1^2\right)t, \left(r - q_2 - \frac{1}{2}\sigma_2^2\right)t, \sigma_1^2 t, \sigma_2^2 t, \rho\right)$$

doi:10.6342/NTU202101125

Since $R^{(m_i)}_{it_{\text{BNJD}}}$ also follows a bivariate normal distribution, we can reconstruct the BS model and define $\hat{R}_{it_{\text{BS}}} := R^{(m_i)}_{it_{\text{BNJD}}}$, where

$$\left(\hat{R}_{1t_{\text{BS}}}, \hat{R}_{2t_{\text{BS}}}\right) \sim \text{BN}\Bigg(\left(r - \hat{q}_1 - \frac{1}{2}\hat{\sigma}_1^2\right)t, \left(r - \hat{q}_2 - \frac{1}{2}\hat{\sigma}_2^2\right)t, \hat{\sigma}_1^2 t, \hat{\sigma}_2^2 t, \hat{\rho}\Bigg)$$

$$(R^{(m_1)}_{1t_{\text{BNJD}}}, R^{(m_2)}_{2t_{\text{BNJD}}}) \sim \text{BN}(\nu_{1t} + m_1\gamma_1, \nu_{2t} + m_2\gamma_2, \sigma_1^2 t + m_1\delta_1^2, \sigma_2^2 t + m_2\delta_2^2, \phi)$$

Hence,

$$\begin{cases} \left(r - \hat{q}_i - \frac{\hat{\sigma}_i^2}{2}\right)t = \left(r - q_i - \lambda_i k_i - \frac{\sigma_i^2}{2}\right)t + m_i\gamma_i \\ \hat{\sigma}_i^2 t = \sigma_i^2 t + m_i\delta_i^2 \\ \hat{\rho} = \phi \end{cases} \tag{3.10}$$

Obtain

$$\begin{cases} \hat{\sigma}_i^2 = \sigma_i^2 + \frac{m_i\delta_i^2}{t} \\ \hat{q}_i = q_i + \Lambda_i k_i - \frac{m_i\gamma_i + \frac{1}{2}m_i\delta_i^2}{t} \\ \hat{\rho} = \phi \end{cases} \tag{3.11}$$

The spread option price of the BNJD can be expressed as the Black-Scholes form

$$\text{ES}_{\text{BNJD}} = \sum_{n_1}\sum_{n_2}\sum_{n_c} p(n_1, n_2, n_c; \lambda_1 t, \lambda_2 t, \lambda_c t)\text{ES}_{\text{BS}}(S_{10}, S_{20}, r, \hat{q}_1, \hat{q}_2, \hat{\sigma}_1, \hat{\sigma}_2, t, \phi) \tag{3.12}$$

After the reconstruction, we can then apply analytical approximations mentioned in Chapter 2 with original formulas under the BS model multiplied by jumping probabilities. Besides, since we calculate the price conditioned on $N_{it} = n_i$, we should add up all the possibilities with three summations.

doi:10.6342/NTU202101125

3.4 Numerical Results

3.4.1 Parameters' Sensitivity

Given equations we just derived, we will examine how parameters affect spread options' prices. In Chapter 3, we still use Simpson's method as benchmark. Different from GBM model in Chapter 2, a jump term is added in the jump-diffusion model so we would examine how volatility (δ_i) of jump size and correlation (ϱ) between jump sizes affect spread options' price. Moreover, we also analyze four different situations which are based on the number of jump frequency (Λ_i) in order to find jump's effect on parameters' sensitivity.

In Table 3.1, we show how parameters of jump affect prices. There are four subtables, each represents a set of jump frequency of both assets. Let's start with the one with high frequency in Table 3.1(a), if we fix mean of jump size at $\gamma = 0.02$, we can observe that prices change little under different values of first asset's volatility (σ_1). From $\sigma_1 = 0.1$ to $\sigma_2 = 0.6$, prices increase only by 10.73%. While δ has a huge impact on prices as σ_1 and γ_1 are fixed. From $\delta = 0.1$ to $\delta = 0.6$, prices increase by 156.24% as σ_1 and γ_1 are fixed. Besides, it's obvious that both mean and variance of jump and volatility have positive impacts on spread options' prices. In Table 3.1 (d), we then discuss the situation of low jump frequency, if we fix $\delta = 0.1$ and $\gamma_1 = 0.1$, the magnitude of prices change has increased.

doi:10.6342/NTU202101125

From $\sigma_1 = 0.1$ to $\sigma_1 = 0.6$, prices increase by 110.76%. Therefore, we can draw the conclusion that the higher the jump frequency, the smaller the impact of parameters of diffusion on prices. Besides, we also find that volatility of jump size is indeed an important parameter to spread options.

Next we are going to examine how correlation of jump size affect spread options' prices. Again, we display four situations from high frequency to low frequency of jump in Table 3.2. We first show the situation under high jump frequency. In Table 3.2(a), if we fix $\eta = 0.3$ and $\rho = -0.5$, the price decreases from 72.184067 at $\varrho = -0.8$ to 64.382277 at $\varrho = 0.8$, which decreases by 10.8%. If we fix $\eta = 0.6$ and $\rho = -0.5$, the price decreases from 75.020651 at $\varrho = -0.8$ to 58.838520 at $\varrho = 0.8$, which decreases by 21.6%. Thus we can make conclusions that correlation of jump size (ϱ) has negative impact on spread options' prices. Moreover, when correlation of jump frequency (η) becomes bigger, the effect is even more obvious. However, if we fix ϱ and η, we find that correlation between underlying assets has tiny effect on prices, prices decrease by only 0.27% from $\rho = -0.5$ to $\rho = 0.5$. We then examine the situation of low jump frequency. In Table 3.2(d), fixing $\varrho = -0.8$ and $\eta = 0.3$, prices decline by 6.82%. We prove again that the higher the jump frequency is, the less impact of diffusion's parameters on spread options. In this table, we also find that, as the sign of ϱ changes, the impact of η on prices would reverse.

We now take a further look at volatility of jump (δ) and correlation of jump size (ϱ)'s comprehensive influence on spread options' prices. In Table 3.3, we demonstrate prices for a wide range value of δ and ϱ. At first sight, we can see that both parameters' effects are positive. Moreover, as δ increases, the effect of ϱ becomes less obvious. We can compare from the opposite of columns. At $\delta = 0.9$, we can observe that prices change little from

doi:10.6342/NTU202101125

$\varrho = 0.9$ to $\varrho = -0.9$. Yet if $\eta = 0.1$, the price have sharp risen from 28.244237 to 42.656000. However, whether ϱ is large or small, prices change a lot under from $\delta = 0.9$ to $\delta = 0.1$. Therefore, we can conclude that volatility of jump size has greater impact on prices than correlation.

Table 3.1: How parameters of jump affect spread options' prices

(a) $\Lambda_1 = 40$, $\Lambda_2 = 20$

	$\delta = 0.1$			$\delta = 0.3$			$\delta = 0.6$		
γ_1	0.02	0.04	0.06	0.02	0.04	0.06	0.02	0.04	0.06
$\sigma_1 = 0.1$	35.516043	36.289513	37.596937	63.881367	64.731030	65.755744	91.006239	91.315288	91.623820
$\sigma_1 = 0.3$	36.103065	36.860814	38.142060	64.087328	64.929454	65.945279	91.026757	91.334167	91.641077
$\sigma_1 = 0.6$	39.327448	40.002817	41.148171	65.263802	66.063651	67.029544	91.146494	91.444386	91.741869

(b) $\Lambda_1 = 10$, $\Lambda_2 = 5$

	$\delta = 0.1$			$\delta = 0.3$			$\delta = 0.6$		
γ_1	0.02	0.04	0.06	0.02	0.04	0.06	0.02	0.04	0.06
$\sigma_1 = 0.1$	18.869395	19.279964	19.983844	35.765658	36.386070	37.144831	65.252781	66.003106	66.790288
$\sigma_1 = 0.3$	20.097102	20.480580	21.138120	36.353278	36.958422	37.699396	65.445594	66.189140	66.969400
$\sigma_1 = 0.6$	26.049948	26.336405	26.830054	39.579587	40.110968	40.764727	66.556763	67.262088	68.003219

(c) $\Lambda_1 = 4$, $\Lambda_2 = 2$

	$\delta = 0.1$			$\delta = 0.3$			$\delta = 0.6$		
γ_1	0.02	0.04	0.06	0.02	0.04	0.06	0.02	0.04	0.06
$\sigma_1 = 0.1$	12.715691	12.965218	13.398176	23.274080	23.712902	24.247590	44.965851	45.642297	46.355748
$\sigma_1 = 0.3$	14.540532	14.756349	15.129630	24.281703	24.689553	25.190777	45.384776	46.049274	46.750657
$\sigma_1 = 0.6$	22.198725	22.335892	22.573909	29.368494	29.680085	30.066803	47.756644	48.356266	48.992618

(d) $\Lambda_1 = 2$, $\Lambda_2 = 1$

	$\delta = 0.1$			$\delta = 0.3$			$\delta = 0.6$		
γ_1	0.02	0.04	0.06	0.02	0.04	0.06	0.02	0.04	0.06
$\sigma_1 = 0.1$	9.840084	9.999959	10.279387	16.727797	17.055478	17.458597	32.451069	33.040069	33.652071
$\sigma_1 = 0.3$	12.130800	12.259511	12.482838	18.211025	18.488489	18.833060	33.089339	33.652544	34.243525
$\sigma_1 = 0.6$	20.738987	20.812772	20.941185	24.810351	24.995760	25.227108	36.795098	37.240383	37.716862

Note:
$S_1 = 100$, $S_2 = 96$, $r = 0.1$, $q_1 = 0.05$, $q_2 = 0.05$, $T = 1$, $\sigma_2 = 0.2$ $\rho = 0.6$, $\gamma_2 = 0.02$, $\varrho = 0.6$, $\eta = 0.4$

3.4.2 Pricing Errors' Analysis under Merton's Jump-Diffusion Model

Given equations we just derived, we would like to compare the accuracy and efficiency between four analytical methods and one numerical integration method. Focus of

doi:10.6342/NTU202101125

Table 3.2: How correlation of jump size affects spread options' prices

(a) $\Lambda_1 = 40, \Lambda_2 = 20$

	$\varrho = -0.8$			$\varrho = 0.2$			$\varrho = 0.8$		
ρ	-0.5	0	0.5	-0.5	0	0.5	-0.5	0	0.5
$\eta = 0$	68.825588	68.733805	68.641597	68.825588	68.733805	68.641597	68.825588	68.733805	68.641597
$\eta = 0.3$	72.184067	72.107092	72.029781	67.706113	67.609063	67.511552	64.382277	64.268974	64.155092
$\eta = 0.6$	75.020651	74.955536	74.890151	66.521467	66.418693	66.315417	58.838520	58.695063	58.550763

(b) $\Lambda_1 = 10, \Lambda_2 = 5$

	$\varrho = -0.8$			$\varrho = 0.2$			$\varrho = 0.8$		
ρ	-0.5	0	0.5	-0.5	0	0.5	-0.5	0	0.5
$\eta = 0$	39.969982	39.682437	39.391677	39.969982	39.682437	39.391677	39.969982	39.682437	39.391677
$\eta = 0.3$	42.544584	42.281026	42.014736	39.100091	38.802443	38.501301	36.700383	36.374579	36.044497
$\eta = 0.6$	44.928365	44.685665	44.440626	38.198591	37.889917	37.577424	32.976045	32.598379	32.214621

(c) $\Lambda_1 = 4, \Lambda_2 = 2$

	$\varrho = -0.8$			$\varrho = 0.2$			$\varrho = 0.8$		
ρ	-0.5	0	0.5	-0.5	0	0.5	-0.5	0	0.5
$\eta = 0$	26.848176	26.352544	25.844170	26.848176	26.352544	25.844170	26.848176	26.352544	25.844170
$\eta = 0.3$	28.441081	27.970285	27.487737	26.248111	25.736064	25.210005	24.698463	24.148283	23.581140
$\eta = 0.6$	29.965234	29.517240	29.058509	25.627389	25.097047	24.551243	22.322073	21.699975	21.054061

(d) $\Lambda_1 = 2, \Lambda_2 = 1$

	$\varrho = -0.8$			$\varrho = 0.2$			$\varrho = 0.8$		
ρ	-0.5	0	0.5	-0.5	0	0.5	-0.5	0	0.5
$\eta = 0$	20.165754	19.451372	18.695304	20.165754	19.451372	18.695304	20.165754	19.451372	18.695304
$\eta = 0.3$	21.140176	20.441172	19.698183	19.738137	18.999670	18.213631	18.717899	17.937462	17.102936
$\eta = 0.6$	22.087880	21.402195	20.669134	19.296639	18.531119	17.710623	17.157857	16.296005	15.362578

Note:
$S_1 = 100$, $S_2 = 96$, $r = 0.1$, $q_1 = 0.05$, $q_2 = 0.05$, $T = 1$, $\sigma_1 = 0.2$, $\sigma_2 = 0.1$, $\delta_1 = 0.3$, $\delta_2 = 0.2$, $\gamma_1 = 0.025$, $\gamma_2 = 0.02$,

Table 3.3: Parameters' sensitivity specified in correlation and volatility

ϱ	δ_1								
	0.9	0.8	0.7	0.6	0.5	0.4	0.3	0.2	0.1
0.9	92.720672	89.564973	84.254576	76.516926	66.496632	54.809818	42.668598	32.401443	28.244237
0.7	93.043976	90.239605	85.443652	78.349632	69.029491	57.995356	46.297750	35.897137	30.337303
0.5	93.318193	90.819653	86.477430	79.956132	71.259959	60.800136	49.476192	38.954674	32.254392
0.3	93.551267	91.319714	87.379376	81.371184	73.237794	63.295395	52.304148	41.684569	34.028587
0.1	93.749736	91.751839	88.168715	82.622665	75.001334	65.532652	54.848256	44.155607	35.683315
-0.1	93.919006	92.126040	88.861364	83.733314	76.580949	67.550886	57.155978	46.414582	37.235974
-0.3	94.063565	92.450680	89.470609	84.721934	78.001226	69.380570	59.262779	48.495266	38.699946
-0.5	94.187156	92.732782	90.007626	85.604245	79.282408	71.046142	61.196113	50.423104	40.085818
-0.7	94.292907	92.978268	90.481873	86.393515	80.441394	72.567593	62.977826	52.217903	41.402153
-0.9	94.383439	93.192152	90.901397	87.101030	81.492450	73.961542	64.625682	53.895480	42.656000

Note:
$S_1 = 100$, $S_2 = 96$, $K = 4$, $r = 0.1$, $q_1 = 0.05$, $q_2 = 0.05$, $\sigma_1 = 0.2$, $\sigma_2 = 0.1$, $T = 1$, $\rho = 0.5$, $\Lambda_1 = 20$, $\Lambda_2 = 20$, $\eta = 0.6$ $\gamma_1 = 0.025$, $\gamma_2 = 0.02$, $\delta_2 = 0.2$

doi:10.6342/NTU202101125

this chapter is to find impacts on pricing errors with jump term added. In this section, we use parameters below as our benchmark: $S_1 = 100, S_2 = 96, r = 0.1, q_1 = 0.05, q_2 = 0.05, \sigma_1 = 0.2, \sigma_2 = 0.2, T = 1, \lambda_1 = 40, \lambda_2 = 20.$

There are six subfigures in Figure 3.1, each displays five pricing errors' curves of discussed methods between different parameters. The green line with cross which represents Gauss-Hermite Quadrature method is almost horizontal in six subfigures which means pricing errors of GHQ are close to zero at each situation. From Figure 3.1, we also find that there are errors which can't be ignored generated by existed approximation methods. Except green line with cross, other curves deviate from zero and fluctuate with change of parameters. From Figure 3.1, we draw a preliminary conclusion that GHQ is the best method to price spread options under Merton's jump-diffusion model.

We then give detailed numbers of pricing errors in Table 3.4. In this table, we display pricing errors of four existed analytical methods and GHQ's method under different value of parameters. Pricing errors are defined as approximation prices minus exact prices. In the table, we can see more clearly that pricing errors of analytical methods are far bigger than pricing errors generated from GHQ.

doi:10.6342/NTU202101125

In addition, we can see from first row to fifth row, as jump frequency of asset 1 (Λ_1) increases, not only spread options' prices rise but pricing errors becomes larger. Similarly, moving on to the sixth row, the impact of volatility of jump size (δ) is also positive, which is as same as the volatility of assets (σ). As for GHQ, when we choose $M = 40$, most pricing errors of GHQ are smaller than 10^{-8} which proves again that GHQ is better than other approximations under MJD.

In Table 3.4(b), there are exact prices and pricing errors between ϱ and η. These two parameters are correlation for each jump frequency and jump size so we should pay much attention to the effect on accuracy. Between different value of correlations, GHQ's errors are still less than 10^{-6} under most situations. Yet most pricing errors generated by analytical approximations are larger than 10^{-3} which can not be ignore. We then confirm that GHQ is the best method among these five pricing engines.

3.4.3 Further Investigation of Gauss-Hermite Quadrature

Now that we find Gauss-Hermite Quadrature are superior to other analytical methods, we would like to take further discussion of GHQ. What we are going to investigate are numbers of grid choosing calculating time and parameters' sensitivity.

doi:10.6342/NTU202101125

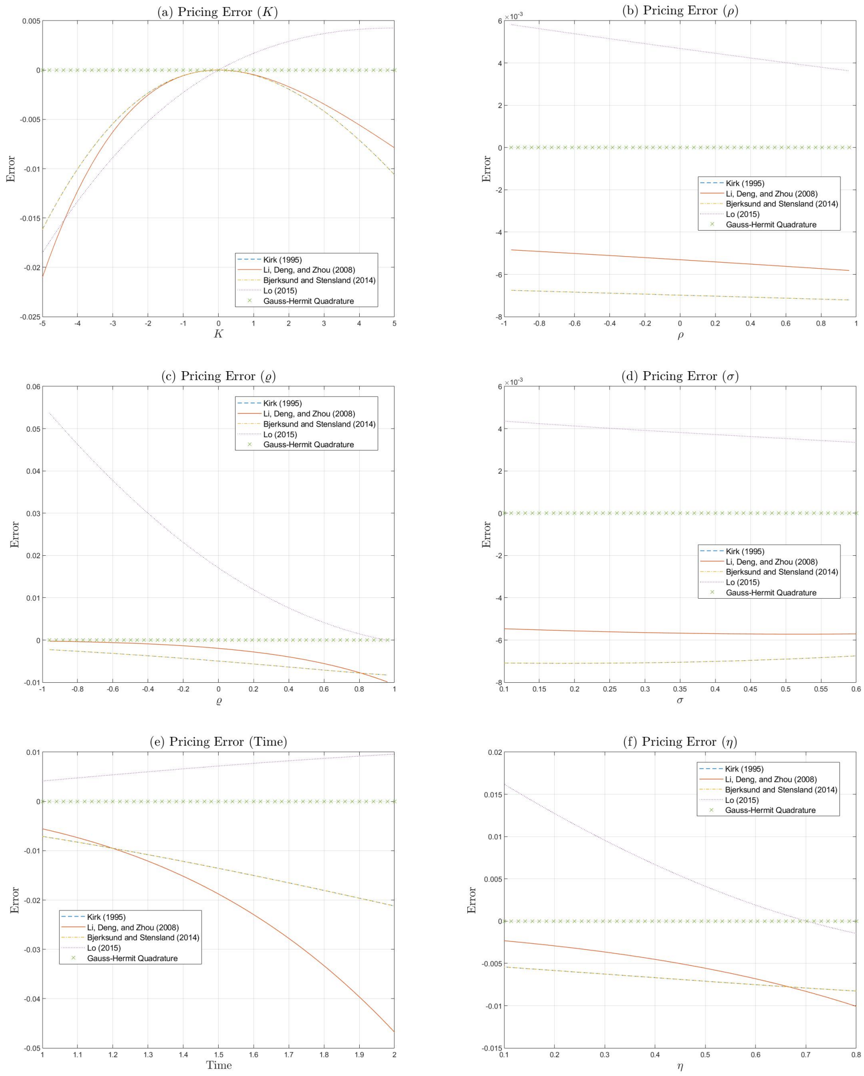

Figure 3.1: Pricing errors' analysis of different pricing methods

doi:10.6342/NTU202101125

Table 3.4: Spread options' prices and pricing errors

(a)

	Exact	Analytical Approximation				GHQ			
	Simpson	Kirk	Li, Deng and Zhou	BjSt	Lo	$M=10$	$M=20$	$M=40$	$M=60$
$\Lambda_1=10$	40.191271	6.1136×10^{-3}	3.9515×10^{-3}	6.1136×10^{-3}	2.1610×10^{-3}	-5.4982×10^{-6}	2.8303×10^{-7}	1.4403×10^{-8}	-3.5115×10^{-10}
$\Lambda_1=20$	49.495722	6.5973×10^{-3}	5.0056×10^{-3}	6.5973×10^{-3}	-3.9370×10^{-3}	-4.9432×10^{-10}	-6.3949×10^{-14}	5.7639×10^{-11}	-1.7689×10^{-9}
$\Lambda_1=30$	56.873493	5.3908×10^{-3}	4.8757×10^{-3}	5.3908×10^{-3}	-2.3599×10^{-3}	-1.3741×10^{-10}	-7.2475×10^{-13}	1.2947×10^{-10}	-5.3728×10^{-9}
$\Lambda_1=40$	62.796597	4.2079×10^{-3}	4.4402×10^{-3}	4.2079×10^{-3}	-8.2204×10^{-4}	-7.5408×10^{-10}	-1.3074×10^{-12}	2.1198×10^{-10}	-1.1554×10^{-8}
$\Lambda_1=50$	67.632228	3.2804×10^{-3}	3.9638×10^{-3}	3.2804×10^{-3}	1.3039×10^{-4}	-8.8883×10^{-10}	-1.7764×10^{-12}	2.9971×10^{-10}	-2.0351×10^{-8}
$\delta_1=0.1$	34.450275	3.7461×10^{-3}	1.8273×10^{-3}	3.7461×10^{-3}	3.0010×10^{-2}	1.1491×10^{-4}	1.6741×10^{-8}	-3.3822×10^{-12}	-3.8543×10^{-10}
$\delta_1=0.2$	47.471932	6.7592×10^{-3}	4.9503×10^{-3}	6.7592×10^{-3}	-2.6773×10^{-3}	-3.6981×10^{-10}	-9.9476×10^{-14}	3.4241×10^{-11}	-8.5483×10^{-10}
$\delta_1=0.3$	62.796597	4.2079×10^{-3}	4.4402×10^{-3}	4.2079×10^{-3}	-8.2204×10^{-4}	-7.5408×10^{-10}	-1.2861×10^{-12}	2.1200×10^{-10}	-1.1554×10^{-8}
$\delta_1=0.4$	75.861694	1.9410×10^{-3}	2.9890×10^{-3}	1.9410×10^{-3}	5.6976×10^{-4}	-5.2080×10^{-10}	-2.9132×10^{-12}	5.4408×10^{-10}	-6.3721×10^{-8}
$\delta_1=0.5$	85.184072	7.8193×10^{-4}	1.7548×10^{-3}	7.8193×10^{-4}	1.0079×10^{-4}	6.0229×10^{-9}	-4.3201×10^{-12}	1.0145×10^{-9}	-2.5133×10^{-7}
$\delta_1=0.6$	90.808364	2.7786×10^{-4}	8.9607×10^{-4}	2.7786×10^{-4}	-4.7419×10^{-4}	2.9613×10^{-7}	-4.4764×10^{-12}	1.5001×10^{-9}	-9.4253×10^{-7}
$\sigma_1=0.1$	62.679022	4.2441×10^{-3}	4.4273×10^{-3}	3.7461×10^{-3}	-9.3473×10^{-4}	-7.3319×10^{-10}	-1.2506×10^{-12}	2.0621×10^{-10}	-1.1024×10^{-8}
$\sigma_1=0.2$	62.796597	4.2079×10^{-3}	4.4402×10^{-3}	6.7592×10^{-3}	-8.2204×10^{-4}	-7.5408×10^{-10}	-1.3074×10^{-12}	2.1198×10^{-10}	-1.1554×10^{-8}
$\sigma_1=0.3$	63.039300	4.1507×10^{-3}	4.4319×10^{-3}	4.2079×10^{-3}	-7.1250×10^{-4}	-7.7597×10^{-10}	-1.3358×10^{-12}	2.1854×10^{-10}	-1.2157×10^{-8}
$\sigma_1=0.4$	63.403327	4.0734×10^{-3}	4.4025×10^{-3}	1.9410×10^{-3}	-6.0692×10^{-4}	-7.9762×10^{-10}	-1.3785×10^{-12}	2.2590×10^{-10}	-1.2837×10^{-8}
$\sigma_1=0.5$	63.883087	3.9776×10^{-3}	4.3526×10^{-3}	7.8193×10^{-4}	-5.0600×10^{-4}	-8.1769×10^{-10}	-1.4140×10^{-12}	2.3409×10^{-10}	-1.3598×10^{-8}
$\sigma_1=0.6$	64.471418	3.8652×10^{-3}	4.2832×10^{-3}	2.7786×10^{-4}	-4.1036×10^{-4}	-8.3492×10^{-10}	-1.4779×10^{-12}	2.4302×10^{-10}	-1.4441×10^{-8}

(b)

	Exact	Analytical Approximation				GHQ			
	(Simpson)	Kirk	LDZ	BjSt	Lo	$M=10$	$M=20$	$M=40$	$M=60$
$\varrho=+0.9$	45.434028	7.4854×10^{-3}	8.1267×10^{-3}	7.4854×10^{-3}	-4.0635×10^{-4}	-8.8147×10^{-10}	-6.0396×10^{-13}	1.6124×10^{-10}	-1.1468×10^{-8}
$\varrho=+0.7$	48.213505	6.9179×10^{-3}	5.8989×10^{-3}	6.9179×10^{-3}	-2.5513×10^{-3}	-4.3178×10^{-10}	-2.1316×10^{-13}	8.4142×10^{-11}	-3.2312×10^{-9}
$\varrho=+0.5$	50.715723	6.2658×10^{-3}	4.2357×10^{-3}	6.2658×10^{-3}	-5.5245×10^{-3}	-4.5467×10^{-10}	7.8160×10^{-14}	3.7772×10^{-11}	-1.0536×10^{-9}
$\varrho=+0.3$	52.990823	5.5945×10^{-3}	3.0052×10^{-3}	5.5945×10^{-3}	-9.3135×10^{-3}	3.5958×10^{-9}	1.9895×10^{-13}	1.3266×10^{-11}	-6.3417×10^{-10}
$\varrho=+0.1$	55.074844	4.9371×10^{-3}	2.1031×10^{-3}	4.9371×10^{-3}	-1.3942×10^{-2}	5.1974×10^{-8}	1.2790×10^{-13}	2.0890×10^{-12}	-7.8288×10^{-10}
$\varrho=-0.1$	56.994955	4.3104×10^{-3}	1.4485×10^{-3}	4.3104×10^{-3}	-1.9428×10^{-2}	4.7035×10^{-7}	-5.5422×10^{-13}	-1.6627×10^{-12}	-1.2862×10^{-9}
$\varrho=-0.3$	58.772355	3.7224×10^{-3}	9.7951×10^{-4}	3.7224×10^{-3}	-2.5775×10^{-2}	2.9759×10^{-6}	-2.4301×10^{-12}	-5.0449×10^{-13}	-2.2685×10^{-9}
$\varrho=-0.5$	60.424034	3.1759×10^{-3}	6.4864×10^{-4}	3.1759×10^{-3}	-3.2973×10^{-2}	9.8183×10^{-6}	1.0652×10^{-10}	5.8051×10^{-12}	-4.1308×10^{-9}
$\varrho=-0.7$	61.963902	2.6710×10^{-3}	4.1943×10^{-4}	2.6710×10^{-3}	-4.1003×10^{-2}	-2.9211×10^{-5}	-4.6530×10^{-9}	1.8510×10^{-11}	-7.8239×10^{-9}
$\varrho=-0.9$	63.403542	2.2063×10^{-3}	2.6404×10^{-4}	2.2063×10^{-3}	-4.9835×10^{-2}	-6.6742×10^{-4}	-7.7346×10^{-7}	1.3252×10^{-11}	-1.5722×10^{-8}
$\eta=+0.9$	42.440969	7.8951×10^{-3}	1.0953×10^{-2}	7.8951×10^{-3}	2.2799×10^{-3}	-1.3847×10^{-9}	-1.1369×10^{-12}	2.1701×10^{-10}	-1.6265×10^{-8}
$\eta=+0.8$	44.379725	7.6331×10^{-3}	9.0755×10^{-3}	7.6331×10^{-3}	1.3739×10^{-3}	-4.6362×10^{-10}	-8.7397×10^{-13}	1.6374×10^{-10}	-9.4166×10^{-9}
$\eta=+0.7$	46.192109	7.3189×10^{-3}	7.4818×10^{-3}	7.3189×10^{-3}	-3.0509×10^{-6}	-2.8507×10^{-11}	-6.6791×10^{-13}	1.1988×10^{-10}	-5.3811×10^{-9}
$\eta=+0.6$	47.893320	6.9694×10^{-3}	6.1365×10^{-3}	6.9694×10^{-3}	-1.7875×10^{-3}	-7.3612×10^{-12}	-4.5475×10^{-13}	8.4889×10^{-11}	-3.0591×10^{-9}
$\eta=+0.5$	49.495722	6.5973×10^{-3}	5.0056×10^{-3}	6.5973×10^{-3}	-3.9370×10^{-3}	-4.9432×10^{-10}	-6.3949×10^{-14}	5.7639×10^{-11}	-1.7689×10^{-9}
$\eta=+0.4$	51.009533	6.2124×10^{-3}	4.0581×10^{-3}	6.2124×10^{-3}	-6.4224×10^{-3}	-1.389×10^{-9}	6.3238×10^{-13}	3.7112×10^{-11}	-1.0944×10^{-9}
$\eta=+0.3$	52.443323	5.8217×10^{-3}	3.2668×10^{-3}	5.8217×10^{-3}	-9.2232×10^{-3}	-1.5024×10^{-9}	1.7621×10^{-12}	2.2162×10^{-11}	-7.8893×10^{-10}
$\eta=+0.2$	53.804362	5.4308×10^{-3}	2.6084×10^{-3}	5.4308×10^{-3}	-1.2324×10^{-2}	3.3044×10^{-9}	3.5314×10^{-12}	1.1710×10^{-11}	-7.1257×10^{-10}
$\eta=+0.1$	55.098889	5.0436×10^{-3}	2.0628×10^{-3}	5.0436×10^{-3}	-1.5713×10^{-2}	2.3202×10^{-8}	6.0325×10^{-12}	4.7677×10^{-12}	-7.9249×10^{-10}

Note:

(a) $S_1=100$, $S_2=96$, $r=0.1$, $q_1=0.05$, $q_2=0.05$, $\sigma_1=0.2$, $\sigma_2=0.1$, $T=1$, $\rho=0.5$, $\Lambda_2=20$, $\gamma_1=-0.05$, $\gamma_2=-0.02$, $\delta_2=0.3$, $\varrho=0.6$, $\eta=0.4$

(b) $S_1=100$, $S_2=96$, $r=0.1$, $q_1=0.05$, $q_2=0.05$, $\sigma_1=0.2$, $\sigma_2=0.1$, $T=1$, $\rho=0.5$, $\Lambda_1=20$, $\Lambda_2=20$, $\gamma_1=-0.05$, $\gamma_2=-0.02$, $\delta_1=0.2$, $\delta_2=0.3$

doi:10.6342/NTU202101125

First, when using Gauss-Hermite Quadrature, we have to decide how many sample points we are going to use. This is a trade-off between accuracy and efficiency. Though the more sample points we use, the more precise results are, we would have to wait longer for results in the mean time. Remember that in Chapter 2 we find that if we choose twenty sample points, we could have stable and accurate results. Since we use a more complicated model in this chapter, we would examine the issue again. As in Figure 3.2, there are six graphs each showed four curves represented GHQ's pricing errors under chosen number of sample points. Comparing these six graphs, it is obviously that the dotted curve represented $M = 20$ fluctuates when maturity being short and when strike being negative. As we choose $M = 40$, the curve is almost horizontal, falling near zero and overlapping with the curve of $M = 60$. In Figure 3.2, we can give preliminary conclusion that when using GHQ under MJD, $M = 40$ should be enough.

Having discussed the influence of single variable on pricing errors of four choices of grids, we then move on to the impact of dual variables on pricing errors. In Figure 3.3, we specifically focus on two most influential parameters which are correlation of jump size (ϱ) and correlation of jump frequency (η). In Figure 3.3, we can observe more clearly the interaction to errors of two correlations and find that correlation of jump size seems to have bigger impacts on pricing errors. Besides, choosing sample points under twenty, pricing errors are larger than 10^{-6}. Again, we prove that choosing forty grids is necessary when we consider using the jump-diffusion model on pricing spread options.

doi:10.6342/NTU202101125

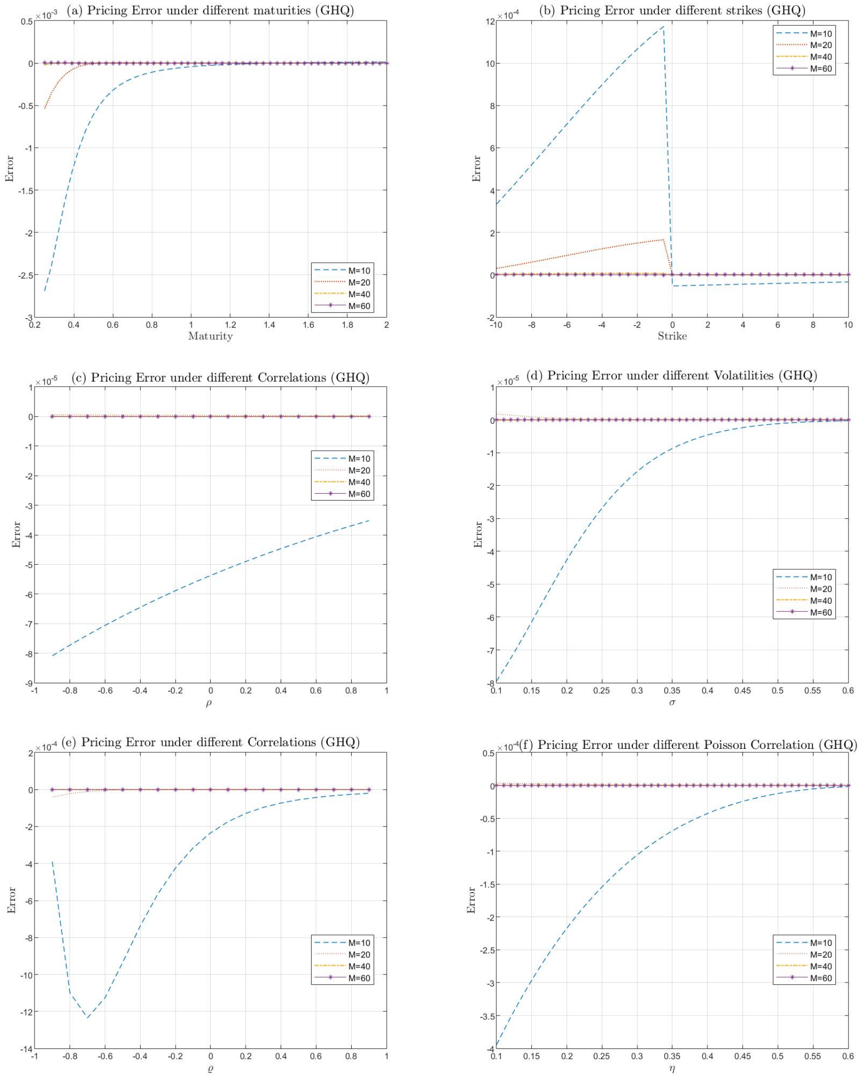

Figure 3.2: Pricing errors' analysis under GHQ

doi:10.6342/NTU202101125

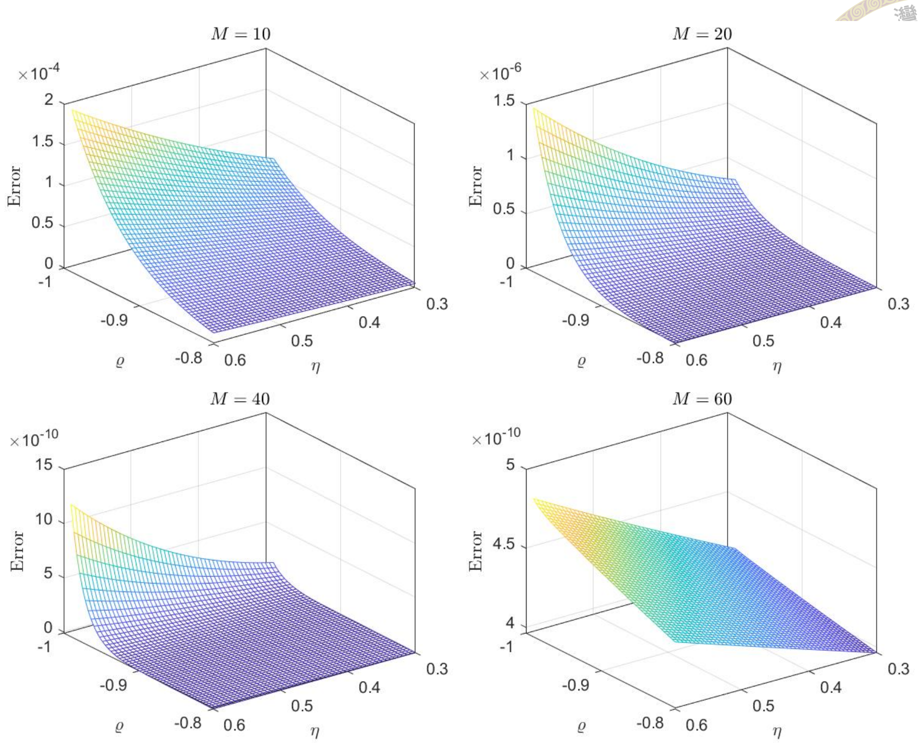

Figure 3.3: Errors' analysis within two parameters using GHQ

After discussing the accuracy of GHQ method, what follows is examination of calculating time of GHQ. The difference of calculating time between different model and different method is highlighted in Table 3.5. We display calculating time comparison not only between analytical approximations and numerical integration, but we also compare calculating time between using Merton's jump-diffusion model and using the Black-Scholes model. First row of the table shows the time we need when pricing under MJD and second row are results as same as in Chapter 2. It can be obtained that calculating time under MJD is at least 3000 times longer than under GBM when using analytical approximations. However, under GHQ, the calculating time under MJD is up to 1000 times longer than that under GBM. Based on the conclusion we just made, choosing $M = 40$ is a relatively safe choice, we can find that calculating time is up to three times longer than approximations and much shorter than Simpson's rule.

doi:10.6342/NTU202101125

In Figure 3.4, we show pictures of ratio of calculating time based on LDZ and Simpson's method. Take Simpson's for example. The y-axis represents how many times of calculating time required for GHQ is that of Simpson's which is calculated as $\frac{\text{calculating time of GHQ}}{\text{calculating time of Simpson}}$. The x-axis represents choices of sample points of GHQ. From these two figures, readers can see the difference of computational efficiency immediately. In the above table and figures, we further confirm that GHQ is the best method when considering accuracy and computational efficiency.

Table 3.5: Calculating time comparison

	Calculating time when running for 100 times								
	Simpson	Kirk	Bjerksund and Stensland'	Lo	Li, Deng and Zhou	Gauss-Hermit Quadrature			
	$N = 2000$					$M = 10$	$M = 20$	$M = 40$	$M = 60$
time (s)									
MJD	1194.338740	2.092682	1.985110	2.224677	6.437983	6.286094	11.641416	22.569801	33.562801
GBM	0.025744	0.006680	0.009293	0.007742	0.012715	0.019074	0.018761	0.059977	0.151187

Note:
$S_1 = 100$, $S_2 = 96$, $r = 0.1$, $q_1 = 0.05$, $q_2 = 0.05$, $\sigma_1 = 0.2$, $\sigma_2 = 0.1$, $T = 1$, $\rho = 0.5$, $\Lambda_1 = 40$, $\Lambda_2 = 20$, $\gamma_1 = -0.05$, $\gamma_2 = -0.02$, $\delta_1 = 0.2$, $\delta_2 = 0.3$, $\varrho = 0.6$, $\eta = 0.4$

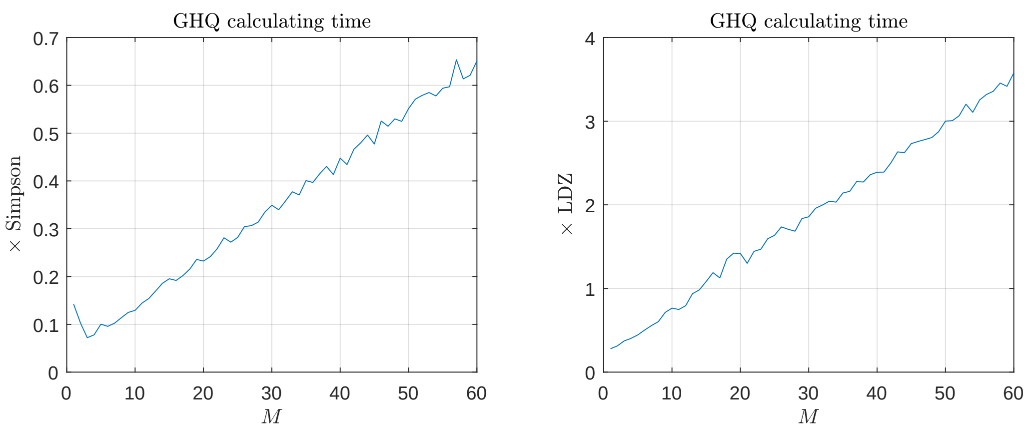

Figure 3.4: GHQ calculating time compared to Simpson and LDZ under MJD

doi:10.6342/NTU202101125

3.5 Conclusions

In Chapter 3, we review Merton's jump-diffusion model, extend the equations on correlated assets, determine the best method under Merton's model and analyze parameters' sensitivity. Below are our findings. For parameters' sensitivity, we find that when a jump term is added, parameters of diffusion model like, volatility, time and correlation between underlying assets have little effect on prices. On the contrary, parameters of the jump term, like correlation and volatility of Poisson process, have great impacts on prices. After we apply analytical approximations and Gauss-Hermite Quadrature mentioned in Chapter 2 on spread options under Merton's model, we analyze the accuracy and computational efficiency between different methods and find that those analytical approximations have large errors. Thus, under the jump-diffusion model, it's inappropriate to use approximations. Instead, GHQ performs better with its minimal errors and computational ease. Additionally, under the jump-diffusion model, calculating time of GHQ is shorter than that of Simpson's rule. To sum up, GHQ is the relative good choice when we price spread options under Merton's jump-diffusion model.

doi:10.6342/NTU202101125

doi:10.6342/NTU202101125

Chapter 4 Pricing Spread Options under Kou's Jump-Diffusion Model

In Chapter 3, we presented methods of pricing spread options of double assets under Merton's jump-diffusion model. However, to describe dramatic change of jump size volatility, bivariate normal jump-diffusion model seems to be not enough. Moreover, empirical investigations show that apart from volatility smile phenomenon, there's also asymmetric leptokurtic feature that the return distribution of assets may have higher peak and heavier tails. Thus in Chapter 4, we would like to review Kou's jump-diffusion model, which used double exponential distribution to model the dynamics of jump size [12]. Under Kou's jump-diffusion model, the pdf of the model is rather complex thus GHQ or Simpson's rule is not suitable. Therefore, in this chapter, we are going to use fast Fourier transform (FFT) to price spread options. And to fix the flaw of the double exponential distribution whose vertices are not connected, we use the asymmetric Laplace to derive the bivariate equations.

doi:10.6342/NTU202101125

4.1 Introduction of Fast Fourier Transform (FFT)

We first briefly introduce FFT, which is an efficient algorithm for computing the sum:

$$w(k) = \sum_{i=1}^{N} e^{-i\frac{2\pi}{N}(j-1)(k-1)} x(j) \quad \text{for} \quad k = 1, \ldots, N \tag{4.1}$$

where N is typically a power of 2.

One of the biggest advantage of FFT is that as long as characteristic functions are given, we can approximate the prices without knowing the probability density function. In the article written by Carr and Madan in 1999, they showed how vanilla options can be priced as characteristic functions are known [5]. Moreover, they also demonstrated that by inverting the characteristic function, they could obtain options' prices by density function. Following Carr and Madan's conclusion, Dempster and Hong extended the equation to multi-factor case specified in jump-diffusion model in 2000 [7]. The method in Dempster and Hong enables us to apply it in which joint characteristic functions of the underlying assets forming the spread are known analytically. They also proved the convenience of FFT which can be easily applied to different diffusion models only by changing the characteristic function. Thus it doesn't alter the computational time significantly which makes FFT superior to Monte Carlo simulation and PDE. In 2004, Chourdakis extended typical FFT to fractional FFT to improve the calculating efficiency [6]. The papers mentioned above all proved that errors can be made to decay as a negative power of the size N of the grids used in computing FFT. Then Hurd and Zhou gave a numerical integration using FFT to price spread options in a two or higher dimensions in 2009 [9].

doi:10.6342/NTU202101125

In addition, Hurd and Zhou proved that errors decay exponentially in the size of the Fourier grids N rather than decay in polynomial. In 2018, Alfeus and Schlögl expended the idea to two-dimension FFT which can be applied on multi-asset financial securities [1]. Other papers regarding FFT can be referred to Schmelzle, who introduced the theory and application of FFT in 2010 [18] and Andersson's master thesis, which focused on spread options' pricing in 2015 [2]. For those who have zero previous knowledge of FFT, Matsuda organized related information including applications under different models in 2004 [15].

In this thesis, we follow Hurd and Zhou's theory in one-dimensional FFT and Alfeus and Schlögl's equations in two-dimensional FFT to further discuss the pricing issue under bivariate asymmetric Laplace model.

To pick the fitting number of subintervals, we compare pricing errors and calculating time using FFT and GHQ under GBM and MJD in the following table. In Table 4.1, we first show relative errors of two numerical methods. Obviously, under both GBM and MJD, using GHQ enables us to obtain quite precise results. In FFT case, $N = 1024$ is required to get the same accurate result as GHQ and if we pick $N = 2048$, we could reduce errors ten times smaller. However, if we choose $N = 4096$, the relative error did not increase. Looking into calculating time in Table 4.2, the required time of FFT is linear growth. When number of N doubles, the calculating time becomes four times. Thus, considering accuracy and efficiency, we would like to use $N = 2048$ as the benchmark when we use FFT in this chapter. Moreover, we can conclude that under simple models like GBM and MJD, GHQ is a relative good method with efficiency and accuracy and FFT is necessary when we encounter complicated models. Since spread options are written on

doi:10.6342/NTU202101125

dual assets, we would demonstrate formulas of two-dimensional FFT in the following section.

Table 4.1: Pricing errors of GHQ and FFT

	GHQ	FFT				
		No. of Discretisations N				
		$N = 512$	$N = 1024$	$N = 2048$	$N = 4096$	$N = 8192$
MJD	-1.5774×10^{-12}	2.7495×10^{-5}	-1.0516×10^{-12}	-8.0291×10^{-13}	1.7835×10^{-12}	5.0520×10^{-12}
GBM	-6.6791×10^{-12}	1.1611×10^{-5}	1.4477×10^{-12}	-2.4869×10^{-14}	5.0449×10^{-13}	4.2633×10^{-14}

Table 4.2: Calculating time of GHQ and FFT

Calculating time when running for 100 times						
	GHQ	FFT				
		No. of Discretisations N				
time (s)		$N = 512$	$N = 1024$	$N = 2048$	$N = 4096$	$N = 8192$
MJD	20.776404	4.012136	16.476821	66.874417	265.510996	1120.499128
GBM	0.035025	3.245354	14.120798	58.384126	232.109384	956.302261

4.1.1 Spread Option Pricing by Two-Dimensional Fourier Transform

In order to price spread options written on the spread of two underlying assets, we should use two-dimensional fast fourier transform. Before using FFT, reader should have basic concept of characteristic function of random variables. If not, Appendix C should be helpful to have an overview of characteristic function and one-dimensional Fourier transform. Readers can also find definitions of continuous and discrete Fourier transforms in Appendix C. We then demonstrate formulas of pricing spread options by FFT in this section.

doi:10.6342/NTU202101125

European Spread Option

Consider the payoff function of a spread option with strike price $K = 1$ given by

$$P(x_1, x_2) := (e^{x_1} - e^{x_2} - 1)^+ \tag{4.2}$$

For $x_1 > 0$, $e^{x_2} < e^{x_1} - 1$, the payoff function of a spread option with strike price $K > 0$ can be re-written as

$$(S_{1T} - S_{2T} - K)^+ = K(e^{X_{1T}} - e^{X_{2T}} - 1)^+ = KP(X_{1T}, X_{2T}) \tag{4.3}$$

where $X_{it} = \ln\left(\frac{S_{it}}{K}\right)$

Subject to the constraints $e^{x_2} < e^{x_1} - 1$, the double integration of fourier transform of $P(x_1, x_2)$ can be calculated as

$$\hat{P}(u_1, u_2) = \int_{-\infty}^{\infty}\int_{-\infty}^{\infty} e^{-i(u_1x_1+u_2x_2)}\,(e^{x_1} - e^{x_2} - 1)^+\,dx_1\,dx_2 \tag{4.4}$$

$$= \int_0^{\infty} e^{-iu_1x_1}\left(\int_{-\infty}^{\ln(e^{x_1}-1)} e^{-iu_2x_2}[(e^{x_1}-1) - e^{x_2}]\,dx_2\right)dx_1 \tag{4.5}$$

$$= \int_0^{\infty} e^{-iu_1x_1}(e^{x_1}-1)^{1-iu_2}\left(\frac{1}{-iu_2} - \frac{1}{1-iu_2}\right)dx_1 \tag{4.6}$$

$$= \frac{\Gamma(i(u_1+u_2)-1)\Gamma(-iu_2)}{\Gamma(iu_1+1)} \tag{4.7}$$

The damping coefficients $\boldsymbol{\epsilon} = (\epsilon_1, \epsilon_2)$ with $\epsilon_2 > 0$ and $\epsilon_1 + \epsilon_2 < -1$ are introduced in order to achieve a square integrable Fourier representation of the spread option's payoff.

doi:10.6342/NTU202101125

In this thesis, we do not discuss with the adequate choice of damping coefficients since there are lots of literatures discussed the issue.

$$P(x_1,x_2) = \frac{1}{4\pi^2}\int_{-\infty}^{\infty}\int_{-\infty}^{\infty} e^{i((u_1+i\epsilon_1)x_1+(u_2+i\epsilon_2)x_2)}\hat{P}(u_1+i\epsilon_1,u_2+i\epsilon_2)\,du_1\,du_2 \quad (4.8)$$

$$= \frac{1}{4\pi^2}\int\int_{\mathbb{R}^2+i\boldsymbol{\epsilon}} e^{i(u_1x_1+u_2x_2)}\hat{P}(u_1,u_2)\,du_1\,du_2 \quad (4.9)$$

Given $X_{it} = \ln S_{it}$, the joint characteristic function of X_{1T} and X_{2T} is given by

$$\varphi(u_1,u_2) = \mathrm{E}\left[e^{iu_1X_{1T}+iu_2X_{2T}}\right] = e^{iu_1X_{10}+iu_2X_{20}}\Phi(u_1,u_2) \quad (4.10)$$

where $\Phi(u_1,u_2)$ is the joint characteristic function for $\ln\left(\frac{S_{1T}}{S_{10}}\right)$ and $\ln\left(\frac{S_{2T}}{S_{20}}\right)$.

The expected value of payoff with $K=1$ is given by

$$\bar{P}(X_{1T},X_{2T}) = \mathrm{E}\left[(e^{X_{1T}}-e^{X_{2T}}-1)^+\right] \quad (4.11)$$

$$= \mathrm{E}\left[\frac{1}{4\pi^2}\int\int_{\mathbb{R}^2+i\epsilon} e^{i(u_1X_{1T}+u_2X_{2T})}\hat{P}(u_1,u_2)\,du_1\,du_2\right] \quad (4.12)$$

$$= \frac{1}{4\pi^2}\int\int_{\mathbb{R}^2+i\boldsymbol{\epsilon}} \mathrm{E}\left[e^{i(u_1X_{1T}+u_2X_{2T})}\right]\hat{P}(u_1,u_2)\,du_1\,du_2 \quad (4.13)$$

$$= \frac{1}{4\pi^2}\int\int_{\mathbb{R}^2+i\boldsymbol{\epsilon}} e^{i(u_1X_{10}+u_2X_{20})}\Phi(u_1,u_2)\hat{P}(u_1,u_2)\,du_1\,du_2 \quad (4.14)$$

Now compute this double sum over the lattice (given N and $\bar{u}$):

$$\boldsymbol{u}(\boldsymbol{k}) := (u_1(k_1),u_2(k_2)) = \{(-\bar{u}+k_1\eta,-\bar{u}+k_2\eta)\mid k_1,k_2=0,1,\cdots,N-1\} \quad (4.15)$$

where the lattice spacing η is given by $\eta = \frac{2\bar{u}}{N}$ and the reciprocal lattice for real-spacing η^* satisfies the Nyquist criterion, i.e. $\eta^* = \frac{2\pi}{N\eta} = \frac{\pi}{\bar{u}}$. Choose initial values $X_{i0} = \ln S_{i0}$ to

doi:10.6342/NTU202101125

lie on the reciprocal lattice with spacing η^* and width $2\bar{x}$, $\bar{x} = \frac{N\eta^*}{2}$:

$$\boldsymbol{x}(\boldsymbol{\ell}) := (x_1(\ell_1), x_2(\ell_2)) = \{(-\bar{x} + \ell_1\eta^*, -\bar{x} + \ell_2\eta^*) \mid \ell_1, \ell_2 = 0, 1, \cdots, N-1\} \quad (4.16)$$

For any $S_{i0} = e^{X_{i0}}$ with $X_{i0} = x_i(\ell_i)$, we then have the approximation

$$\bar{P}(X_{1T}, X_{2T}) \approx \frac{\eta^2}{4\pi^2} \sum_{k_1=0}^{N-1} \sum_{k_2=0}^{N-1} e^{i(\boldsymbol{u}(\boldsymbol{k})+i\boldsymbol{\epsilon})\boldsymbol{x}(\boldsymbol{\ell})'} \Phi(\boldsymbol{u}(\boldsymbol{k}) + i\boldsymbol{\epsilon}) \hat{P}(\boldsymbol{u}(\boldsymbol{k}) + i\boldsymbol{\epsilon}) \quad (4.17)$$

Now, as usual for the discrete FFT, as long as N is even,

$$i\boldsymbol{u}(\boldsymbol{k})\boldsymbol{x}(\boldsymbol{\ell})' = i\pi(k_1 + k_2 + \ell_1 + \ell_2) + i\frac{2\pi}{N}k_1\ell_1 + i\frac{2\pi}{N}k_2\ell_2 \quad (4.18)$$

With $e^{i\pi} = -1$, this leads to the double inverse discrete Fourier transform

$$\bar{P}(X_{1T}, X_{2T}) \approx (-1)^{\ell_1+\ell_2} \left(\frac{\eta N}{2\pi}\right)^2 e^{-(\epsilon_1 x_1(\ell_1)+\epsilon_2 x_2(\ell_2))} \left[\frac{1}{N^2} \sum_{k_1=0}^{N-1} \sum_{k_2=0}^{N-1} e^{i\frac{2\pi}{N}k_1\ell_1} e^{i\frac{2\pi}{N}k_2\ell_2} H(\boldsymbol{k})\right] \quad (4.19)$$

$$= (-1)^{\ell_1+\ell_2} \left(\frac{\eta N}{2\pi}\right)^2 e^{-(\epsilon_1 x_1(\ell_1)+\epsilon_2 x_2(\ell_2))} \left[\text{ifft2}(H)\right](\boldsymbol{\ell}) \quad (4.20)$$

where

$$H(\boldsymbol{k}) = (-1)^{k_1+k_2} \Phi(\boldsymbol{u}(\boldsymbol{k}) + i\boldsymbol{\epsilon}) \hat{P}(\boldsymbol{u}(\boldsymbol{k}) + i\boldsymbol{\epsilon})$$

The price of a spread option with $K > 0$

$$\Pi^+ = Ke^{-rT}\bar{P}(X_{1T}, X_{2T}) \quad (4.21)$$

For $K < 0$

$$\Pi^- = \Pi^+ Ke^{-rT} - \left(S_{10}e^{-q_1T} - S_{20}e^{-q_2T}\right) \quad (4.22)$$

doi:10.6342/NTU202101125

4.2 Kou's Jump-Diffusion Model

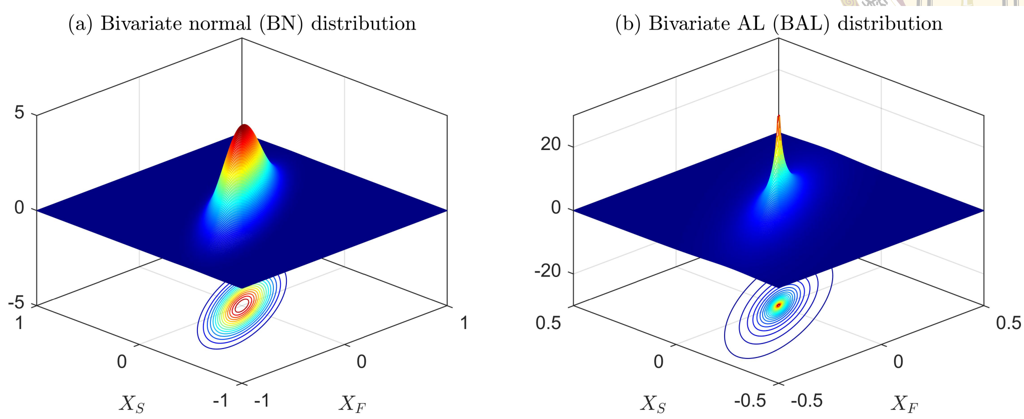

Figure 4.1: BAL v.s. BN

We first review Kou's model in this section [12]. Like Merton's model, there is a jump term in the stochastic differential equation. The difference is that the jump size in Kou's model follows double exponential distribution rather than normal distribution. To demonstrate the BN and BAL distributions, we use figures from Ulyah, Lin and Miao's article in 2018 which discussed pricing short-dated foreign equity options with a bivariate jump-diffusion model with correlated fat-tailed jumps in Figure 4.1 [19]. Figure 4.1 shows the difference between bivariate normal (BN) and bivariate asymmetric Laplace (BAL) distribution. Apparently, BAL is more leptokurtic and fat-tailed than BN. Kou had mentioned in his article that both double exponential and normal jump-diffusion models can lead to leptokurtic feature though the kurtosis from double exponential is significantly more pronounced. In empirical study, markets often overreact or underreact to good or bad news. By the features of double exponential, Kou's model can be used to model both overreaction and underreaction which attribute to fat-tailed and leptokurtic each. In this thesis, one of our purpose is to build a satisfied model to interpret market's reaction. By Kou's assumption, events arrived by a Poisson process, and the asset prices change ac-

doi:10.6342/NTU202101125

cording to the distribution of jump size.

Below are stochastic differential equations of Kou's jump-diffusion model.

$$\frac{dS_t}{S_t} = \mu dt + \sigma dW(t) + d\left(\sum_{i=1}^{N_{(t)}}(V_i - 1)\right) \tag{4.23}$$

where $W(t)$ is a standard browian motion, N(t) is a Poisson process with rate λ and V_i is a sequence of independent identically distributed (i.i.d.) nonnegative random variables such that $\gamma = \log(V)$ has an asymmetric double exponential distribution with the density

$$f_\gamma(y) = p \cdot \eta_1 e^{-\eta_1 y} 1_{\{y\geq 0\}} + q \cdot \eta_2 e^{-\eta_2 y} 1_{\{y<0\}}, \quad \eta_1 > 1, \eta_2 > 1 \tag{4.24}$$

where where $p, q \geq 0$, $p + q = 1$, represent the probabilities of upward and downward jumps. In other words,

$$\log(V) = \gamma \stackrel{d}{=} \begin{cases} \xi^+, & \text{with probability } p \\ \xi^-, & \text{with probability } q \end{cases} \tag{4.25}$$

Though Kou's model proves that double exponential jump-diffusion model leads to closed form solution and maintain the analytical tractability to path-dependent options, Kou only discussed option pricing under single asset. Thus, in this thesis, we would like to use Kou's jump-diffusion model as framework, switch the distribution of jump size to asymmetric Laplace distribution and extended stochastic differential equations to double assets.

doi:10.6342/NTU202101125

4.3 Bivariate Asymmetric Laplace Jump-Diffusion Model

4.3.1 Bivariate Asymmetric Laplace Distribution

According to Kotz, the bivariate asymmetric Laplace distributions constitute a five parameter family of two-dimensional distributions given by the characteristic function [11]

$$\psi_{(X_1,X_2)}(\alpha_1,\alpha_2) = \frac{1}{1+\frac{\omega_1^2\alpha_1^2}{2}+\rho\omega_1\omega_2\alpha_1\alpha_2+\frac{\omega_2^2\alpha_2^2}{2}-i\theta_1\alpha_1-i\theta_2\alpha_2} \tag{4.26}$$

where the five parameters θ_l, θ_2, ω_1, ω_2, and ρ satisfy

$$\theta_1 \in \mathbb{R}, \qquad \theta_2 \in \mathbb{R}, \qquad \omega_1 \geq 0, \qquad \omega_2 \geq 0, \qquad \rho \in [0,1]$$

PDF of BAL

$$\begin{aligned} f(x,y) = & \frac{\exp\left[((\theta_1\omega_2/\omega_1-\theta_2\rho)x+(\theta_2\omega_1/\omega_2-\theta_1\rho)y)/(\omega_1\omega_2(1-\rho^2))\right]}{\pi\omega_1\omega_2\sqrt{1-\rho^2}} \\ & \cdot K_0\left(D\sqrt{x^2\omega_2/\omega_1-2\rho xy+y^2\omega_1/\omega_2}\right) \end{aligned} \tag{4.27}$$

doi:10.6342/NTU202101125

where K_0 is modified Bessel function of the second kind with index 0

$$K_0(z) = \int_0^\infty \cos(z \ \sinh t) dt$$

and

$$D = \frac{\sqrt{2\omega_1\omega_2(1-\rho^2) + \theta_1^2\omega_2/\omega_1 - 2\theta_1\theta_2\rho + \theta_2^2\omega_1/\omega_2}}{\omega_1\omega_2(1-\rho^2)}$$

The marginal distribution $\text{AL}(\theta, \omega)$

$$f_{\text{AL}}(x; \theta, \omega) = \frac{1}{\sqrt{\theta^2 + \omega^2}} \begin{cases} \exp\left(-\frac{2}{\sqrt{\theta^2+2\omega^2}+\theta} x\right) & \text{for } x \geq 0 \\ \exp\left(\frac{2}{\sqrt{\theta^2+2\omega^2}-\theta} x\right) & \text{for } x < 0 \end{cases} \tag{4.28}$$

Compare with the double exponential (DE) distribution $\text{DE}(p, \eta^+, \eta^-)$

$$f_{\text{DE}}(x; \eta^+, \eta^-, p) = \begin{cases} p\eta^+ \exp\left(-\eta^+ x\right) & \text{for } x \geq 0 \\ (1-p)\eta^- \exp\left(\eta^- x\right) & \text{for } x < 0 \end{cases} \tag{4.29}$$

Take DE distribution parametrization (3 parameters) into AL distribution (2 parameters) with an additional condition

$$\lim_{x \to 0^-} f_{\text{DE}}(x) = \lim_{x \to 0^+} f_{\text{DE}}(x) \tag{4.30}$$

Hence, in $f_{\text{DE}}(x)$

$$p = \frac{\eta^-}{\eta^+ + \eta^-}, \qquad q = \frac{\eta^+}{\eta^+ + \eta^-} \tag{4.31}$$

doi:10.6342/NTU202101125

Define AL parametrization $\mathrm{AL}^*(\eta^+, \eta^-)$

$$f_{\mathrm{AL}^*}(x; \eta^+, \eta^-) = \frac{\eta^+\eta^-}{\eta^+ + \eta^-} \begin{cases} \exp(-\eta^+ x) & \text{for } x \geq 0 \\ \exp(\eta^- x) & \text{for } x < 0 \end{cases} \tag{4.32}$$

$$\psi_{\mathrm{AL}^*}(\alpha_1, \alpha_2) = \frac{\eta^+\eta^-}{\eta^+ + \eta^-} \left(\frac{1}{\eta^+ - i\alpha_1} + \frac{1}{\eta^- + i\alpha_2} \right) \tag{4.33}$$

Related to the parametrization $\mathrm{AL}(\theta, \omega)$ through the following formulas:

$$\eta_i^+ = \frac{\sqrt{\theta_i^2 + 2\omega_i^2} - \theta_i}{\omega_i^2} \tag{4.34}$$

$$\eta_i^- = \frac{\sqrt{\theta_i^2 + 2\omega_i^2} + \theta_i}{\omega_i^2} \tag{4.35}$$

or

$$\theta_i = \frac{1}{\eta_i^+} - \frac{1}{\eta_i^-} \tag{4.36}$$

$$\omega_i^2 = \frac{2}{\eta_i^+ \eta_i^-} \tag{4.37}$$

4.3.2 BALJD

With equations of BAL distribution, we can derive formulas of BAL jump-diffusion model (BALJD). Under BALJD, underlying assets are assumed to follow the jump-diffusion model of which the jump size follows fat-tailed distribution. And the return R_{it} of an underlying asset consists of three parts, D_{it}, X_{it} and X_{it}^c.

doi:10.6342/NTU202101125

While diffusion ones are same as in Merton's model, the difference lies on jump term. To distinguish parameters from Chapter 3, we use θ_i and ω_i as mean and variance respectively.

$$R_{it} = \nu_{it} + \sigma_i W_{it} + \sum_{j=1}^{N_{it}} \ln Y_{ij} + \sum_{j=1}^{N_{ct}} \ln Y_{ij}^c = D_{it} + X_{it} + X_{it}^c \tag{4.38}$$

where

$$(D_{1t},\, D_{2t}) \sim \text{BN}\left(\nu_{1t},\, \nu_{2t},\, \sigma_1^2 t, \sigma_2^2\, t,\, \rho\right)$$

$$\nu_{it} = \left(\mu_i - \frac{\sigma_i^2}{2}\right) t$$

$$\mu_i = (r - q_i) - \frac{\ln\left(\text{E}[e^{X_{it}+X_{it}^c}]\right)}{t} = r - q_i - \Lambda_i k_i$$

$$k_i = \text{E}\left[e^{\ln Y_i}\right] - 1 = \frac{1}{1 - \frac{1}{2}\omega_i^2 - \theta_i} - 1$$

$$\ln Y_i \sim \text{AL}(\theta_i, \omega_i)$$

$$(\ln Y_1^c,\, \ln Y_2^c) \sim \text{BAL}\left(\theta_1,\, \theta_2,\, \omega_1, \omega_2,\, \varrho\right)$$

Then the characteristic function of the joint distribution of the return can be written as follows.

$$\varphi(u_1,\, u_2) = \text{E}\left[e^{iu_1 R_1 + iu_2 R_2}\right] = \text{E}\left[e^{iu_1(D_{1t}+X_{1t}+X_{1t}^c)+iu_2(D_{2t}+X_{2t}+X_{2t}^c)}\right] \tag{4.39}$$

$$= \text{E}\left[e^{iu_1 D_{1t}+iu_2 D_{2t}}\right] \text{E}\left[e^{iu_1 X_{1t}}\right] \text{E}\left[e^{iu_2 X_{2t}}\right] \text{E}\left[e^{iu_1 X_{1t}^c + iu_2 X_{2t}^c}\right] \tag{4.40}$$

$$= \varphi_{D_{1t},D_{2t}}(u_1,\, u_2)\varphi_{X_{1t}}(u_1)\varphi_{X_{2t}}(u_2)\varphi_{X_{1t}^c,X_{2t}^c}(u_1,\, u_2) \tag{4.41}$$

doi:10.6342/NTU202101125

where

$$\varphi_{D_{1t},D_{2t}}(u_1,\, u_2) = \exp\left(i(u_1\nu_{1t} + u_2\nu_{2t}) - \frac{1}{2}(u_1^2\sigma_1^2 + u_2^2\sigma_2^2 + 2u_1u_2\sigma_1\sigma_2\rho)t \right)$$

$$\varphi_{X_{it}}(u_i) = \exp\left(\lambda_1 t\left(\varphi_{\ln Y_i}(u_i)\right) - 1\right)$$

$$\varphi_{X_{1t}^c,X_{2t}^c}(u_1,u_2) = \exp\left(\lambda_c t\left(\varphi_{\ln Y_1^c,\ln Y_2^c}(u_1,u_2)\right) - 1\right)$$

$$\varphi_{\ln Y_i}(u_i) = \frac{1}{1+\frac{1}{2}u_i^2\omega_i^2 - iu_i\theta_i}$$

$$\varphi_{\ln Y_1^c,\ln Y_2^c}(u_1,u_2) = \frac{1}{1+\frac{1}{2}u_1^2\omega_1^2 + \varrho u_1u_2\omega_1\omega_2 + \frac{1}{2}u_2^2\omega_2^2 - iu_1\theta_1 - iu_2\theta_2}$$

4.4 Numerical Results

4.4.1 Impact of Jump Term

Since the jump-diffusion model with bivariate asymmetric Laplace distribution is proved to have more pronounced kurtosis, we would like to examine the difference of prices modeled by GBM, Merton's model and the bivariate asymmetric Laplace jump-diffusion model. Before conducting numerical research, we would like to clarify the parameters' setting. To compare two jump-diffusion models, we should fix mean and variance of jump size distribution. As shown in formula C.19 in Appendix C, δ_i^2 equals $\omega_i^2 + \theta_i^2$ and θ_i equals γ_i. We would use these equations to transform parameters between two models in order to obtain the fairest comparison.

doi:10.6342/NTU202101125

As our initial guess, prices under BAL jump-duffusion model should be higher than prices under MJD then GBM. Besides, as we have discussed in section one in this chapter, using fourier grids $N = 2048$ can obtain precise prices with pricing errors within 10^{-12} and can strike a balance between accuracy and computational efficiency. Therefore, we would use fourier grids $N = 2048$ as our benchmark in this section.

In Figure 4.2, we show prices simulated by three models changing under different parameters. We compare prices under maturity, strike, correlation between assets, volatility and both assets. Unsurprisingly, prices under Merton' and BAL model are much higher than prices under GBM at all situations we chose. The result totally makes sense since we use jump term to capture investors' overreaction and underreaction to the market.

After proving our initial guess of jumps' impact on prices, we then narrow down the issue to the comparison between Merton's and BAL JD and two graphs are added to represent the comparison between jumps' parameters. Since mean of jump size (γ_i) being positive or negative controls the trend prices change, we analyze three situations , each are when both γ are positive, both γ are negative and $\gamma_1 > 0, \gamma_2 < 0$. In Figure 4.3, when both assets' γ are fixed to be negative, we can observe that prices by Merton's JD are greater than prices by Kou's JD. Then we move on to the situation when both γ are positive, the result shown in Figure 4.4 reverse from Figure 4.3. Prices by Kou's model are higher than by Merton's model, the magnitude of price difference is even bigger. Finally, because that the spread is defined as $S_1 - S_2$, we set γ_1 to be positive and γ_2 to be negative in order to make spreads bigger. In Figure 4.5, we can see that the result is similar to what in Figure 4.4. Prices by Kou are obviously higher than by Merton's. This result is also reasonable since when $\gamma_1 > 0$, $\gamma_2 < 0$, S_1 would increase and S_2 would decrease over time by which

doi:10.6342/NTU202101125

the spread would become larger and more positive. In addition, the effect of rising prices will also be magnified under Kou's model. In Table 4.3, we show prices modeled by bivariate normal and bivariate asymmetric Laplace jump-diffusion models under different situations so as to make readers more aware of prices' difference.

After confirming the truth that the magnitude of spread options' prices change under Kou's model followed the bivariate asymmetric Laplace distribution indeed much larger, we would like to perform parameters' analysis consequently.

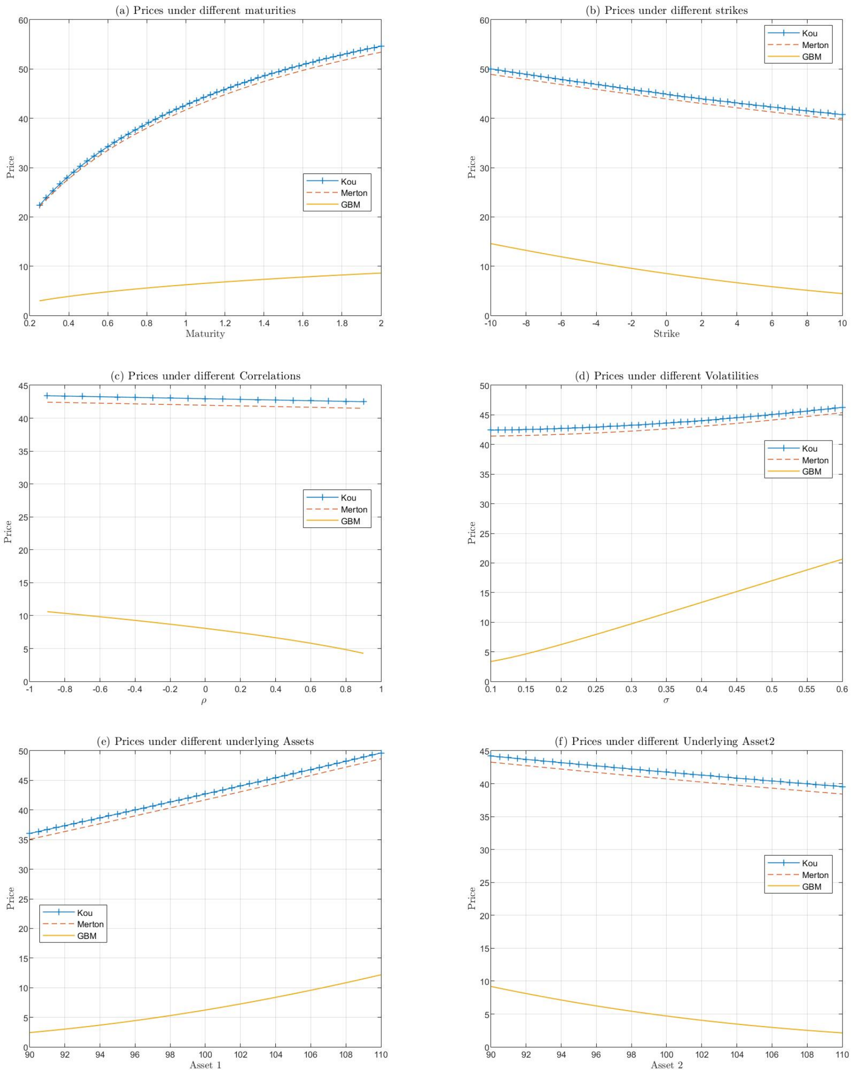

Figure 4.2: Comparison of prices under three models

doi:10.6342/NTU202101125

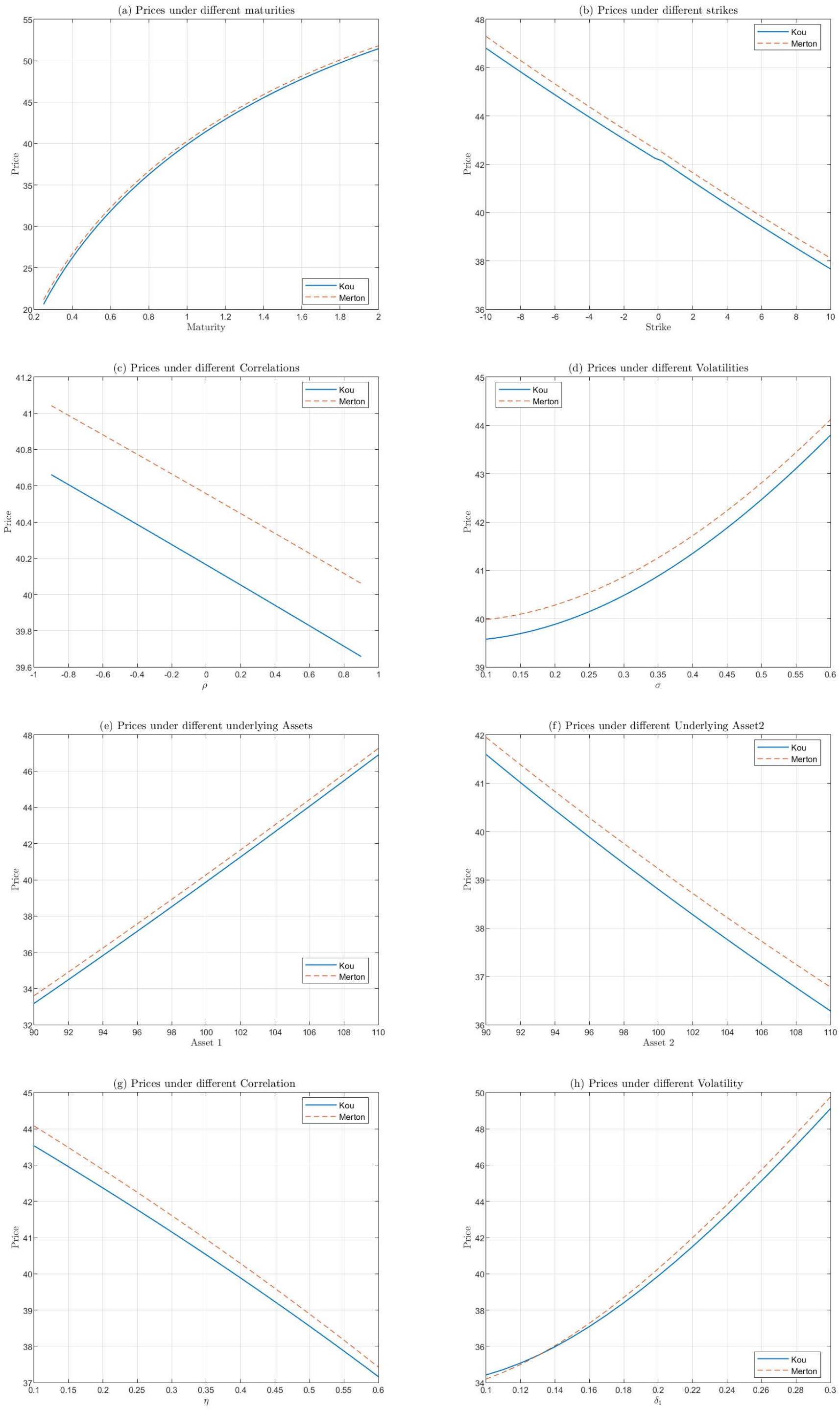

Figure 4.3: Comparison of prices under two JD models(both γ are negative)

doi:10.6342/NTU202101125

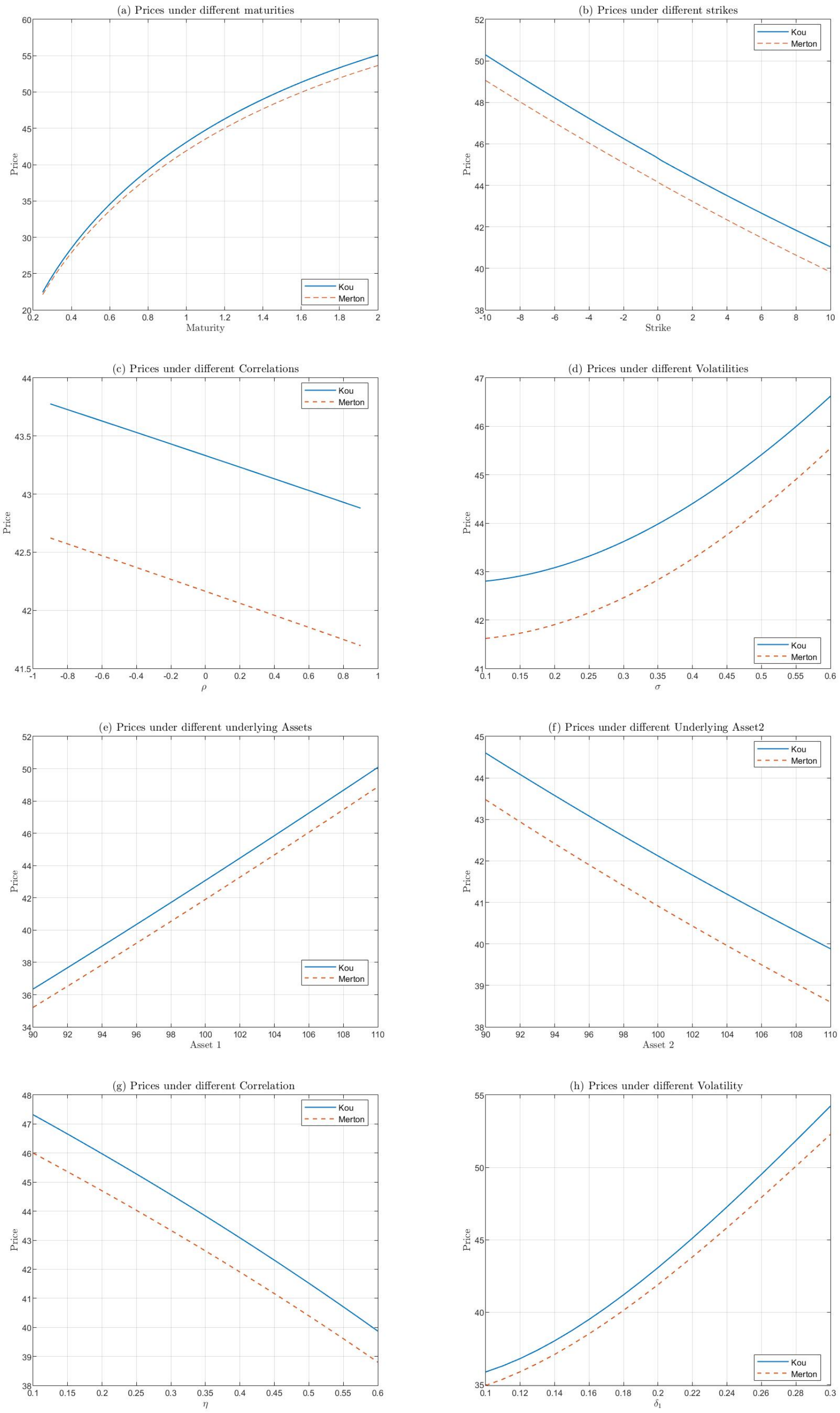

Figure 4.4: Comparison of prices under two JD models(both γ are positive)

doi:10.6342/NTU202101125

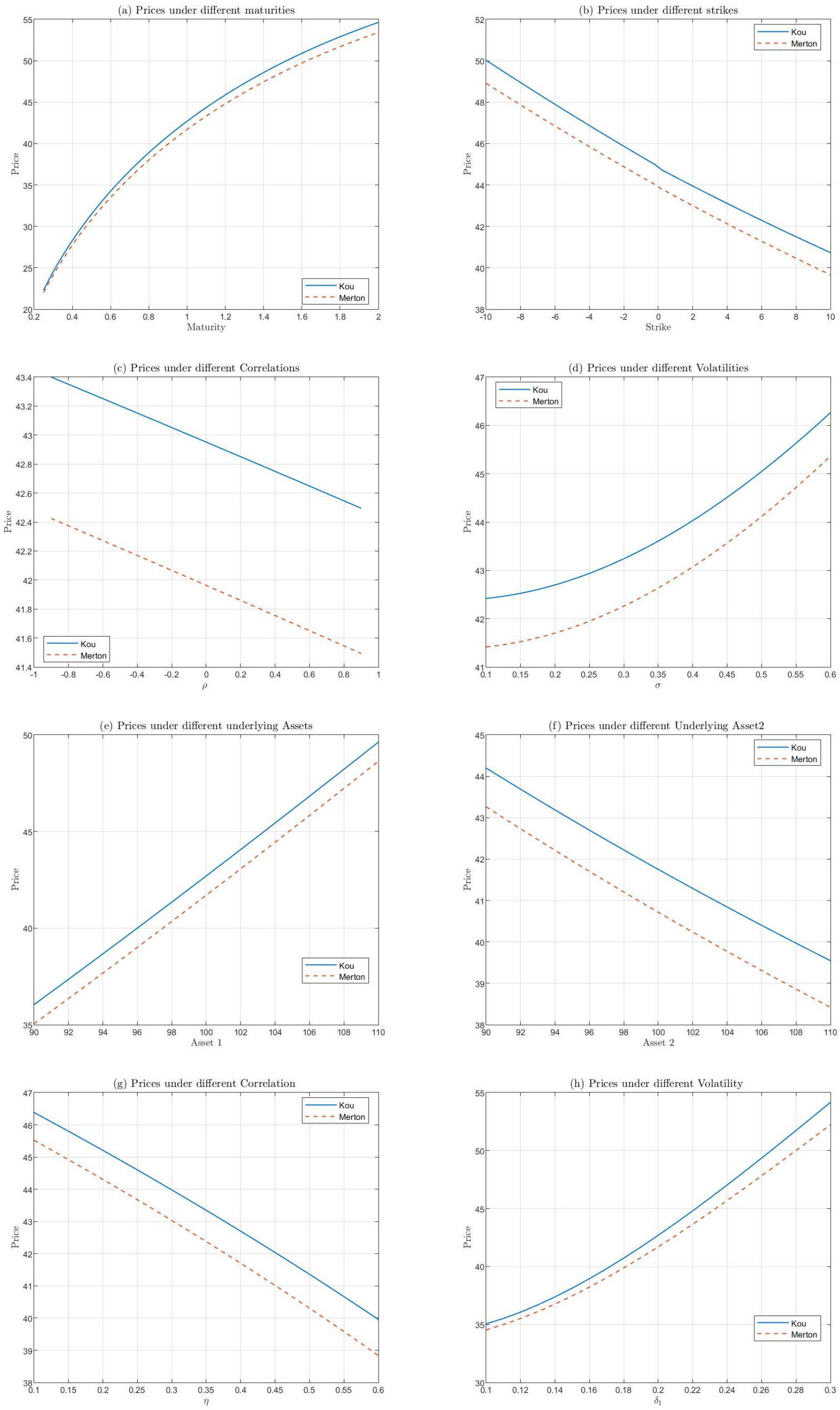

Figure 4.5: Comparison of prices between two JD models($\gamma_1 > 0$, $\gamma_2 < 0$)

doi:10.6342/NTU202101125

Table 4.3: Comparison between BN and BAL jump-diffusion models

	model			model	
parameter	BNJD	BALJD	parameter	BNJD	BALJD
$T = 0.25$	24.969307	25.347037	$S_1 = 96$	43.653157	44.904445
$T = 0.50$	34.660819	35.502378	$S_1 = 98$	45.042127	46.294326
$T = 1.00$	46.440801	47.693534	$S_1 = 100$	46.440801	47.693534
$T = 1.25$	50.472033	51.824772	$S_1 = 102$	47.848900	49.101813
$T = 1.50$	53.737944	55.352860	$S_1 = 104$	49.266159	50.518916
$K = 2$	46.930124	48.155013	$\gamma = -0.025$	45.245060	45.218201
$K = 4$	46.440801	47.693534	$\gamma = -0.015$	45.382808	45.493690
$K = 6$	45.964860	47.245099	$\gamma = -0.010$	45.470895	45.672694
$K = 8$	45.501570	46.808961	$\gamma = +0.015$	46.101539	46.980932
$K = 10$	45.050266	46.384447	$\gamma = +0.025$	46.440801	47.693534
$\rho = -0.4$	46.889509	48.125339	$\delta_1 = 0.01$	24.169682	24.413927
$\rho = -0.2$	46.800367	48.039538	$\delta_1 = 0.03$	28.206365	28.537454
$\rho = +0.2$	46.621188	47.867100	$\delta_1 = 0.05$	33.714442	34.245278
$\rho = +0.4$	46.531146	47.780459	$\delta_1 = 0.07$	39.948260	40.787640
$\rho = +0.6$	46.440801	47.693534	$\delta_1 = 0.09$	46.440801	47.693534
$\sigma_1 = 0.1$	46.222236	47.483194	$\varrho = 0.1$	51.779495	52.966135
$\sigma_1 = 0.2$	46.440801	47.693534	$\varrho = 0.3$	49.778299	50.983809
$\sigma_1 = 0.3$	46.890390	48.126337	$\varrho = 0.5$	47.603352	48.843066
$\sigma_1 = 0.4$	47.559838	48.771170	$\varrho = 0.7$	45.221490	46.483428
$\sigma_1 = 0.5$	48.433291	49.613151	$\varrho = 0.9$	42.586029	43.849494

doi:10.6342/NTU202101125

4.4.2 Parameters' Sensitivity

In this section, we would like to perform parameters' analysis specified in correlations and volatilities. Showed in Table 4.4, we analyze effects of volatility of first asset (σ_1), mean (γ_1) and volatility (δ) of jump size. Similarly, in order to discuss the influence of diffusion parameters under different jump frequency, we conduct four sensitivity analysis from high jump frequency to low jump frequency using the same set of data as in Chapter 3. To see the impact of jumps, we set jump frequency to be higher at $\Lambda_1 = 40$ and $\Lambda_2 = 20$ first. Then we can observe that fixing both assets' volatility, the price rises a lot as δ increases and the rise is even higher than under Merton's jump-diffusion model. In addition, as jump frequency becomes higher, the impact of diffusion parameters are weaker. Same as Merton's model, mean of jump size in Kou's model has positive impact on spread options' prices.

Table 4.5 are results related to correlations' sensitivity. Since prices diverge when $\Lambda_1 = 40$, $\Lambda_2 = 20$, we adjust parameters of jump frequency to $\Lambda_1 = 20$, $\Lambda_2 = 10$ in the first table of Table 4.4. Compared to Table 4.4, it seems like correlations of jump process (η) and correlation of jump size (ϱ) have less impact on spread options' prices than volatilities under BAL jump-diffusion model. Additionally, we can confirm that the prices under BAL JD are higher than Merton's JD through detailed numbers in Table 4.4 and Table 4.5.

doi:10.6342/NTU202101125

In the process of numerical analysis, we found that using FFT under greater volatility and jump frequency, the price might diverge to an extremely large number. Therefore, when using FFT to price spread options under BAL jump-diffusion models, we should pay special attention to the setting of parameters.

Table 4.4: Parameters' sensitivity of jump size

(a) $\Lambda_1 = 40$, $\Lambda_2 = 20$

	$\delta = 0.1$			$\delta = 0.15$			$\delta = 0.2$		
θ_1	0.01	0.03	0.05	0.01	0.03	0.05	0.01	0.03	0.05
$\sigma_1 = 0.1$	34.504241	36.187221	38.946250	40.456384	42.206993	44.831799	47.591862	49.394459	51.877395
$\sigma_1 = 0.2$	34.839053	36.501130	39.229332	40.725535	42.459357	45.061121	47.800692	49.589863	52.055619
$\sigma_1 = 0.3$	35.521870	37.142159	39.808479	41.276552	42.976457	45.531560	48.229587	49.991415	52.422132

(b) $\Lambda_1 = 10$, $\Lambda_2 = 5$

	$\delta = 0.1$			$\delta = 0.15$			$\delta = 0.2$		
θ_1	0.01	0.03	0.05	0.01	0.03	0.05	0.01	0.03	0.05
$\sigma_1 = 0.1$	17.703376	18.639637	20.180828	20.963591	21.967679	23.487426	24.995727	26.090170	27.619346
$\sigma_1 = 0.2$	18.448686	19.336878	20.812667	21.581516	22.548124	24.019870	25.503173	26.567677	28.060888
$\sigma_1 = 0.3$	19.888714	20.699875	22.063630	22.800769	23.702681	25.087669	26.519485	27.529435	28.954988

(c) $\Lambda_1 = 4$, $\Lambda_2 = 2$

	$\delta = 0.1$			$\delta = 0.15$			$\delta = 0.2$		
θ_1	0.01	0.03	0.05	0.01	0.03	0.05	0.01	0.03	0.05
$\sigma_1 = 0.1$	11.228337	11.840242	12.842027	13.263399	13.929385	14.928758	15.770736	16.512111	17.537576
$\sigma_1 = 0.2$	12.453238	12.978097	13.863991	14.302642	14.892180	15.800736	16.646925	17.320851	18.274439
$\sigma_1 = 0.3$	14.580131	15.017463	15.766766	16.182898	16.687876	17.477086	18.287291	18.878451	19.726678

(d) $\Lambda_1 = 2$, $\Lambda_2 = 1$

	$\delta = 0.1$			$\delta = 0.15$			$\delta = 0.2$		
θ_1	0.01	0.03	0.05	0.01	0.03	0.05	0.01	0.03	0.05
$\sigma_1 = 0.1$	8.033244	8.436817	9.115436	9.359724	9.812680	10.507054	10.990350	11.512952	12.246147
$\sigma_1 = 0.2$	9.722000	10.036708	10.577015	10.859718	11.221005	11.787956	12.316118	12.741370	13.354707
$\sigma_1 = 0.3$	12.342316	12.590627	13.020380	13.275913	13.567738	14.028653	14.523568	14.873073	15.380561

Note:
$S_1 = 100$, $S_2 = 96$, $r = 0.1$, $q_1 = 0.05$, $q_2 = 0.05$, $T = 1$, $\sigma_2 = 0.1$, $\rho = 0.6$, $\gamma_2 = -0.02$, $\varrho = 0.6$, $\eta = 0.4$

doi:10.6342/NTU202101125

Table 4.5: Parameters' sensitivity (correlation)

(a) $\Lambda_1 = 20$, $\Lambda_2 = 10$

	$\varrho = -0.8$			$\varrho = 0.2$			$\varrho = 0.8$		
ρ	-0.5	0	0.5	-0.5	0	0.5	-0.5	0	0.5
$\eta = 0$	56.085346	55.927153	55.767986	56.085346	55.927153	55.767986	56.085346	55.927153	55.767986
$\eta = 0.3$	59.135492	58.994778	58.853258	55.328166	55.165297	55.001409	52.604010	52.423362	52.241492
$\eta = 0.6$	61.880161	61.755000	61.627793	54.548957	54.381214	54.212407	48.610104	48.400819	48.189950

(b) $\Lambda_1 = 10$, $\Lambda_2 = 5$

	$\varrho = -0.8$			$\varrho = 0.2$			$\varrho = 0.8$		
ρ	-0.5	0	0.5	-0.5	0	0.5	-0.5	0	0.5
$\eta = 0$	42.045849	41.779522	41.510622	42.045849	41.779522	41.510622	42.045849	41.779522	41.510622
$\eta = 0.3$	44.508219	44.263118	44.015845	41.406092	41.133627	40.858507	39.204372	38.908911	38.610300
$\eta = 0.6$	46.811768	46.585605	46.357601	40.752176	40.473443	40.191990	36.046332	35.714530	35.378789

(c) $\Lambda_1 = 4$, $\Lambda_2 = 2$

	$\varrho = -0.8$			$\varrho = 0.2$			$\varrho = 0.8$		
ρ	-0.5	0	0.5	-0.5	0	0.5	-0.5	0	0.5
$\eta = 0$	27.994571	27.522603	27.041878	27.994571	27.522603	27.041878	27.994571	27.522603	27.041878
$\eta = 0.3$	29.496135	29.047829	28.592643	27.532584	27.051490	26.562150	26.102251	25.589524	25.066805
$\eta = 0.6$	30.953579	30.528630	30.098974	27.061507	26.571566	26.074405	24.057955	23.496122	22.923011

(d) $\Lambda_1 = 2$, $\Lambda_2 = 1$

	$\varrho = -0.8$			$\varrho = 0.2$			$\varrho = 0.8$		
ρ	-0.5	0	0.5	-0.5	0	0.5	-0.5	0	0.5
$\eta = 0$	20.723802	20.017697	19.278903	20.723802	20.017697	19.278903	20.723802	20.017697	19.278903
$\eta = 0.3$	21.612753	20.921997	20.200482	20.376011	19.652969	18.896091	19.448765	18.690602	17.893487
$\eta = 0.6$	22.488735	21.813402	21.109788	20.020020	19.279072	18.503411	18.100778	17.282141	16.416658

Note:
$S_1 = 100$, $S_2 = 96$, $r = 0.1$, $q_1 = 0.05$, $q_2 = 0.05$, $T = 1$, $\sigma_1 = 0.2$, $\sigma_2 = 0.1$, $\delta_1 = 0.3$, $\delta_2 = 0.2$, $\gamma_1 = 0.05$, $\gamma_2 = -0.02$,

doi:10.6342/NTU202101125

4.5 Conclusions

In Chapter 4, we not only review how Fast Fourier method can be applied on derivatives pricing, but also use Kou's model replaced with bivariate asymmetric Laplace distribution to derive equations. Moreover, we compare prices under three models mentioned in this thesis. As we prove by figures, features of fat-tailed and leptokurtic are able to strengthen the extent of prices increasing so we can make our first conclusion that jump-diffusion under fat-tailed distribution should be able to capture investors' sentiment in the market. Second, under the BAL jump-diffusion model, using the fast Fourier transform should be an eligible method to strike a balance between efficiency and accuracy.

doi:10.6342/NTU202101125

Chapter 5 Conclusions and Future Work

5.1 Conclusions

In this thesis, we not only list widespread analytical approximations, but we review Merton's and Kou's jump-diffusion models and extend them to the bivariate distributions so that we can apply on spread options. Moreover, we improve the drawbacks of Kou's model and extend his formula to correlated assets' pricing. Through rigorous analysis, we then give suggestions of best pricing method under the Black-Scholes model, Merton's and Kou's jump-diffusion models. To sum up, under the Black-Scholes model, LDZ and GHQ are comparable. While under Merton's jump-diffusion model, though analytical approximations seem to take less time, yet the pricing errors are too large to be ignored. To strike a balance between accuracy and efficiency, Gauss-Hermite quadrature is the best method under Merton's jump-diffusion model. To ensure efficiency, we even discussed the perfect number of sample points of GHQ which is forty sample points. Finally, under Kou's jump-diffusion model, we use fast Fourier transform to price spread options since the probability density functions of fat-tailed distributions are complicated. And because

doi:10.6342/NTU202101125

FFT can be used as long as we have characteristic functions. We also pick the most suitable number of sample points considering accuracy and calculating efficiency.

5.2 Future Work

This thesis sorts different kinds of pricing engines for spread options. However, we did not conduct empirical research to confirm if the prices generated by models discussed in this article to be align with market prices. Also, since spread options are often traded at over-the-counter market, we can not reach out the data to calibrate the parameters. Therefore, subsequents can conduct empirical research and calibrate models' parameters if market data be available. Moreover, since Greeks are one of the most indispensable parts of hedging, follow-up researchers can also conduct in-depth research in this area.

doi:10.6342/NTU202101125

References

[1] Mesias Alfeus and Erik Schlögl. On numerical methods for spread options splitting method. In *QUANTITATIVE FINANCE RESEARCH CENTRE*. 2018.

[2] Max Andersson. Valuation of spread options using the fast fourier transform under stochastic volatility and jump diffusion models. In *Lund University Faculty of engineering*. 2015.

[3] Teodora Baeva. On the pricing and sensitivity of spread options on two correlated assets. In *SSRN Electronic Journal*. 2010.

[4] Petter Bjerksund and Gunnar Stensland. Closed form spread option valuation. In *Quantitative Finance*, volume 14 of *10*, page 1785–1794. Norway, 2011.

[5] Peter Carr, Morgan Stanley, and Dilip Madan. Option valuation using the fast fourier transform. In *Journal of Computational Finance*, volume 2. 1999.

[6] Kyriakos Chourdakis. Option pricing using the fractional fft. In *Journal of Computational Finance*, volume 4. 2005.

[7] M. A. H. Dempster and S. S. G. Hong. Spread option valuation and the fast

doi:10.6342/NTU202101125

fourier transform. In *Mathematical Finance—Bachelier Congress*, pages 203–220. Springer, Berlin, Heidelberg, 2002.

[8] John C. Hull. *OPTIONS, FUTURES,AND OTHER DERIVATIVES*. Pearson Education, 9th edition, 2015.

[9] Thomas Hurd and Zhuowei Zhou. A fourier transform method for spread option pricing. In *SIAM Journal on Financial Mathematics*, pages 142–157. 2010.

[10] E. Kirk. Correlation in the energy markets. In *Managing Energy Price Risk*, pages 71–78. Risk Publications, 1995.

[11] Samuel Kotz, TomaszJ. Kozubowski, and Krzysztof Podgörski. *The Laplace Distribution and Generalizations*. Springer Science+Business Media, LLC, 1th edition, 2001.

[12] SG Kou. A jump-diffusion model for option pricing. In *Management Science*, volume 48, pages 1086–1101. 2002.

[13] Minqiang Li, ShiJie Deng, and JieYun Zhou. Closed-form approximations for spread option prices and greeks. In *The Journal of Derivatives*, pages 58–80. NewYork, 2008.

[14] Chi Fai Lo. Pricing spread options by the operator splitting method. In *WILMOTT magazine*, pages 64–67. 2015.

[15] Kazuhisa Matsuda. Introduction to option pricing with fourier transform: Option pricing with exponential lévy models. In *Department of Economics The Graduate Center, The City University of New York*. 2004.

doi:10.6342/NTU202101125

[16] Robert C. Merton. Option pricing when underlying stock returns are discontinuous. In *Journal of Financial Economics*, volume 3, pages 125–144. 1976.

[17] William H. Press, Saul A. Teukolsky, William T. Vetterling, and Brian P. Flannery. *Numerical Recipes in C*. Press Syndicate of the University of Cambridge, 2th edition, 2002.

[18] Martin Schmelzle. Option pricing formulae using fourier transform: Theory and application. 2010.

[19] Siti Maghfirotul Ulyah, Xenos Chang-Shuo Lin, and Daniel Wei-Chung Miao. Pricing short-dated foreign equity options with a bivariate jump-diffusion model with correlated fat-tailed jumps. In *Finance Research Letters*, volume 24, pages 113–128. 2018.

[20] Jente Van Belle, Steven Vanduffel, and Jing Yao. Closed-form approximations for spread options in lévy markets. In *Applied Stochastic Models in Business and Industry*, volume 35. 2018.

doi:10.6342/NTU202101125

doi:10.6342/NTU202101125

Appendix A — Bivariate Distributions

A.1 Bivariate Normal Distribution (BN)

First of all, we would like to introduce some basic sets of bivariate Normal distribution.

Two random variables X and Y are said to have a bivariate normal distribution.

$$(X, Y) \sim \text{BN}(\mu_X, \sigma_X^2, \mu_Y, \sigma_Y^2, \rho) \tag{A.1}$$

Their joint PDF is given by

$$f_{XY}(x, y) = \frac{1}{2\pi\sigma_X\sigma_Y\sqrt{1-\rho^2}}\exp\left(-\frac{1}{2(1-\rho^2)}\left[\left(\frac{x-\mu_X}{\sigma_X}\right)^2+\left(\frac{y-\mu_Y}{\sigma_Y}\right)^2-2\rho\frac{(x-\mu_X)(y-\mu_Y)}{\sigma_X\sigma_Y}\right]\right) \tag{A.2}$$

The marginal PDF of X and Y are

$$f_X(x) = \int_{-\infty}^{\infty} f_{XY}(x, y)dy = f_N(x; \mu_X, \sigma_X^2), \quad f_Y(y) = \int_{-\infty}^{\infty} f_{XY}(x, y)dx = f_N(y; \mu_Y, \sigma_Y^2) \tag{A.3}$$

The conditional PDF of X given Y is

$$f_{X|Y=y}(x|y) = \frac{f_{XY}(x, y)}{f_Y(y)} = f_N\left(x; \mu_X + \frac{\sigma_X}{\sigma_Y}\rho(y-\mu_Y), (1-\rho^2)\sigma_X^2\right) \tag{A.4}$$

doi:10.6342/NTU202101125

A.2 Bivariate Poisson Distribution (BP)

Next, we would display basic sets of bivariate Poisson distribution. As mentioned before, we separate jump frequency M_i into independent one denoted N_i and joint one denoted N_c. Therefore, we can model the bivariate Poisson distribution that denotes

$$M_i = N_i + N_c, \quad i = 1, 2 \tag{A.5}$$

where

$$N_i \sim \text{Pois}(\lambda_i) \tag{A.6}$$

$$N_c \sim \text{Pois}(\lambda_c) \tag{A.7}$$

$$\Lambda_i = \lambda_i + \lambda_c \tag{A.8}$$

We said (M_1, M_2) follow a bivariate distribution with mean Λ_1, Λ_2 and correlation η.

$$(M_1, M_2) \sim \text{BP}(\Lambda_1, \Lambda_2, \eta) \tag{A.9}$$

doi:10.6342/NTU202101125

where the correlation can be calculated as

$$\eta = \text{Corr}(M_1, M_2) = \frac{\text{Cov}(M_1, M_2)}{\sqrt{\text{Var}(M_1)\text{Var}(M_2}} \tag{A.10}$$

$$= \frac{\text{Cov}(N_1, N_2) + \text{Cov}(N_1, N_c) + \text{Cov}(N_2, N_c) + \text{Cov}(N_c, N_c)}{\sqrt{\text{Var}(M_1)Var(M_2)}} \tag{A.11}$$

$$= \frac{\text{Var}(N_c)}{\sqrt{\big(\text{Var}(N_1) + \text{Var}(N_c)\big)\big(\text{Var}(N_2) + \text{Var}(N_c)\big)}} \tag{A.12}$$

$$= \frac{\lambda_c}{\sqrt{\Lambda_1 \Lambda_2}} \tag{A.13}$$

Then the joint mass function of (M_1, M_2) can be expressed as

$$\Pr(M_1 = m_1, M_2 = m_2) = \sum_{\substack{n_1+n_c=m_1 \\ n_2+n_c=m_1}} \text{p}(n_1, n_2, n_c) \tag{A.14}$$

where

$$\text{p}(n_1, n_2, n_c) = \Pr\big(N = (n_1, n_2, n_c)\big) = \frac{e^{-(\lambda_1+\lambda_2+\lambda_c)}\lambda_1^{n_1}\lambda_2^{n_2}\lambda_c^{n_c}}{n_1!n_2!n_c!} \tag{A.15}$$

doi:10.6342/NTU202101125

doi:10.6342/NTU202101125

Appendix B — Option Pricing under Jump-Diffusion Models

B.1 European Vanilla Call Option

The price of a call option in the BS model can be written as

$$\mathrm{EC}_{\mathrm{BS}}\big(S_0, K, r, q, \sigma, t\big) = e^{-rt}\mathrm{E}\big[(S_0 e^{R_{t_{\mathrm{BS}}}} - K)^+\big] \tag{B.16}$$

where $R_{t_{\mathrm{BS}}} = (r - q - \frac{1}{2}\sigma^2)t + \sigma W_t$ and $R_{t_{\mathrm{BS}}} \sim \mathcal{N}\big((r - q - \frac{1}{2}\sigma^2)t, \sigma^2 t\big)$.

The price of MJD model can be expressed as

$$\mathrm{EC}_{\mathrm{MJD}} = e^{-rt}E\big[(S_0 e^{R_{t_{\mathrm{MJD}}}} - K)^+\big] = e^{-rt}\sum_{n=0}^{\infty} f_{\mathrm{Pois}}(n; \lambda t)\mathrm{E}\Big[(S_0 e^{R^{(n)}_{t_{\mathrm{MJD}}}} - K)^+\Big] \tag{B.17}$$

Since $R^{(n)}_{t_{\mathrm{MJD}}}$ also follows a normal distribution, we can reconstruct the BS model and define $\hat{R}_{t_{\mathrm{BS}}} := R^{(n)}_{t_{\mathrm{MJD}}}$, where

$$\hat{R}_{t_{\mathrm{BS}}} \sim \mathcal{N}\left(\left(\hat{r} - q - \frac{1}{2}\hat{\sigma}^2\right)t, \hat{\sigma}^2 t\right) \tag{B.18}$$

doi:10.6342/NTU202101125

We have

$$R_{t_{\text{MJD}}}^{(n)} \sim \mathcal{N}\left(\left(r - q - \frac{\sigma^2}{2} - \lambda k\right)t + n\gamma, \sigma^2 t + n\delta^2\right) \tag{B.19}$$

Hence,

$$\begin{cases} \left(\hat{r} - q - \frac{\hat{\sigma}^2}{2}\right)t = \left(r - q - \frac{\sigma^2}{2} - \lambda k\right)t + n\eta \\ \hat{\sigma}^2 t = \sigma^2 t + n\delta^2 \end{cases} \tag{B.20}$$

Obtain

$$\begin{cases} \hat{r} = r - \lambda k + \frac{n\gamma + \frac{1}{2}n\delta^2}{t} \\ \hat{\sigma}^2 = \sigma^2 + \frac{n\delta^2}{t} \end{cases} \tag{B.21}$$

The call option price of MJD can be expressed as BS form

$$\text{EC}_{\text{MJD}}(S_0, K, r, q, \sigma, t, \lambda, \gamma, \delta) = e^{-rt}\sum_{n=0}^{\infty} f_{\text{Pois}}(n; \lambda t)\text{E}\left[(S_0 e^{\hat{R}_{\text{BS}}} - K)^+\right] \tag{B.22}$$

$$= \sum_{n=0}^{\infty} f_{\text{Pois}}(n; \lambda t) e^{-(r-\hat{r})t} e^{-\hat{r}t}\text{E}\left[(S_0 e^{\hat{R}_{\text{BS}}} - K)^+\right] \tag{B.23}$$

$$= \sum_{n=0}^{\infty} f_{\text{Pois}}(n; \lambda t) e^{-(r-\hat{r})t}\text{EC}_{\text{BS}}(S_0, K, \hat{r}, q, \hat{\sigma}, t) \tag{B.24}$$

doi:10.6342/NTU202101125

Appendix C — Characteristic Function and FFT

C.1 Characteristic Function

Normal

If $X \sim \mathcal{N}(\mu,\, \sigma^2)$

$$\varphi(u) = \mathrm{E}\left[e^{iuX}\right] = \exp\left(iu\mu - u^2\sigma^2/2\right) \tag{C.25}$$

Bivariate Normal

If $(X_1,\, X_2) \sim \mathrm{BN}(\mu_1,\, \mu_2,\, \sigma_1^2,\, \sigma_2^2,\, \rho)$

$$\varphi(u_1,\, u_2) = \mathrm{E}\left[e^{iu_1X_1 + iu_2X_2}\right] = \exp\left(i(u_1\mu_1 + u_2\mu_2) - \frac{1}{2}(u_1^2\sigma_1^2 + u_2^2\sigma_2^2 + 2u_1u_2\sigma_1\sigma_2\rho)\right) \tag{C.26}$$

doi:10.6342/NTU202101125

Asymmetric Laplace

If $X \sim \text{AL}(\theta,\, \omega)$

$$\varphi(u) = \text{E}\left[e^{iuX}\right] = \frac{1}{1 + \frac{1}{2}u^2\omega^2 - iu\theta} \tag{C.27}$$

$$\text{E}[X] = \theta \qquad \text{Var}(X) = \omega^2 + \theta^2 \tag{C.28}$$

Bivariate Asymmetric Laplace

If $(X_1,\, X_2) \sim \text{BAL}(\theta_1,\, \theta_2,\, \omega_1,\, \omega_2,\, \rho)$

$$\varphi(u_1,\, u_2) = \text{E}\left[e^{iu_1X_1 + iu_2X_2}\right] = \frac{1}{1 + \frac{1}{2}u_1^2\omega_1^2 + \rho u_1 u_2 \omega_1 \omega_2 + \frac{1}{2}u_2^2\omega_2^2 - iu_1\theta_1 - iu_2\theta_2} \tag{C.29}$$

Compound Poisson

If $Y \sim \sum_{j=1}^{N} X_j$

$$\varphi_Y(u) = e^{\lambda(\varphi_X(u) - 1)} \tag{C.30}$$

C.2 Geometric Brownian Motion (GBM)

$$R_{it} = \nu_{it} + \sigma_i W_{it} \tag{C.31}$$

doi:10.6342/NTU202101125

where

$$\nu_{it} = \left(\mu_i - \frac{\sigma_i^2}{2}\right) t \tag{C.32}$$

$$\mu_i = r - q_i \tag{C.33}$$

$$(\sigma_1 W_{1t}, \sigma_2 W_{2t}) \sim \text{BN}\left(0,\ 0,\ \sigma_1^2 t, \sigma_2^2\, t,\ \rho\right) \tag{C.34}$$

$$\varphi(u_1,\ u_2) = \text{E}\left[e^{iu_1 R_1 + iu_2 R_2}\right] = \exp\left(i(u_1\nu_{1t} + u_2\nu_{2t}) - \frac{1}{2}(u_1^2\sigma_1^2 + u_2^2\sigma_2^2 + 2u_1u_2\sigma_1\sigma_2\rho)t\right) \tag{C.35}$$

doi:10.6342/NTU202101125

C.3 Bivariate Normal Jump-Diffusion (BNJD)

$$R_{it} = \nu_{it} + \sigma_i W_{it} + \sum_{j=1}^{N_{it}} \ln Y_{ij} + \sum_{j=1}^{N_{ct}} \ln Y_{ij}^c = D_{it} + X_{it} + X_{it}^c \tag{C.36}$$

where

$$(D_{1t},\, D_{2t}) \sim \text{BN}\left(\nu_{1t},\, \nu_{2t},\, \sigma_1^2 t, \sigma_2^2\, t,\, \rho\right) \tag{C.37}$$

$$\nu_{it} = \left(\mu_i - \frac{\sigma_i^2}{2}\right) t \tag{C.38}$$

$$\mu_i = (r - q_i) - \frac{\ln\left(\text{E}[e^{X_{it}+X_{it}^c}]\right)}{t} = r - q_i - \Lambda_i k_i \tag{C.39}$$

$$k_i = \text{E}\left[e^{\ln Y_i}\right] - 1 = e^{\gamma_i + \frac{1}{2}\delta_i^2} - 1 \tag{C.40}$$

$$\ln Y_i \sim \mathcal{N}(\gamma_i, \delta_i^2) \tag{C.41}$$

$$(\ln Y_1^c,\, \ln Y_2^c) \sim \text{BN}\left(\gamma_1,\, \gamma_2,\, \delta_1^2, \delta_2^2,\, \varrho\right) \tag{C.42}$$

$$\varphi(u_1,\, u_2) = \text{E}\left[e^{iu_1 R_1 + iu_2 R_2}\right] = \text{E}\left[e^{iu_1(D_{1t}+X_{1t}+X_{1t}^c)+iu_2(D_{2t}+X_{2t}+X_{2t}^c)}\right] \tag{C.43}$$

$$= \text{E}\left[e^{iu_1 D_{1t}+iu_2 D_{2t}}\right] \text{E}\left[e^{iu_1 X_{1t}}\right] \text{E}\left[e^{iu_2 X_{2t}}\right] \text{E}\left[e^{iu_1 X_{1t}^c + iu_2 X_{2t}^c}\right] \tag{C.44}$$

$$= \varphi_{D_{1t},D_{2t}}(u_1,\, u_2)\varphi_{X_{1t}}(u_1)\varphi_{X_{2t}}(u_2)\varphi_{X_{1t}^c,X_{2t}^c}(u_1,\, u_2) \tag{C.45}$$

doi:10.6342/NTU202101125

where

$$\varphi_{D_{1t},D_{2t}}(u_1,\, u_2) = \exp\left(i(u_1\nu_{1t} + u_2\nu_{2t}) - \frac{1}{2}(u_1^2\sigma_1^2 + u_2^2\sigma_2^2 + 2u_1u_2\sigma_1\sigma_2\rho)t \right) \tag{C.46}$$

$$\varphi_{X_{it}}(u_i) = \exp\left(\lambda_1 t\left(\varphi_{\ln Y_i}(u_i)\right) - 1\right) \tag{C.47}$$

$$\varphi_{X_{1t}^c,X_{2t}^c}(u_1, u_2) = \exp\left(\lambda_c t\left(\varphi_{\ln Y_1^c,\ln Y_2^c}(u_1, u_2)\right) - 1\right) \tag{C.48}$$

$$\varphi_{\ln Y_i}(u_i) = \exp\left(iu_i\gamma_i - \frac{1}{2}u_i^2\delta_i^2 \right) \tag{C.49}$$

$$\varphi_{\ln Y_1^c,\ln Y_2^c}(u_1, u_2) = \exp\left(i(u_1\gamma_1 + u_2\gamma_2) - \frac{1}{2}(u_1^2\delta_1^2 + u_2^2\delta_2^2 + 2u_1u_2\delta_1\delta_2\varrho) \right) \tag{C.50}$$

C.4 One-Dimensional Fourier Transform

Continuous Fourier Transform (CFT)

The Fourier transform of f is defined as follows:

$$\mathcal{F}[f](u) := \hat{f}(u) = \int_{-\infty}^{\infty} e^{iux}\, f(x)\, dx, \quad \forall u \in \Re \tag{C.51}$$

The inverse of a Fourier transform is given by the Fourier inversion formula:

$$f(x) = \frac{1}{2\pi}\int_{-\infty}^{\infty} e^{-iux}\, \hat{f}(u)\, du \tag{C.52}$$

doi:10.6342/NTU202101125

The characteristic function of a continuous univariate random variable, with its probability density function f, is defined as a Fourier transform of its PDF,

$$\hat{f}(u) := \psi(u) \tag{C.53}$$

Discrete Fourier Transform (DFT)

For complex numbers $g_0, \ldots, g_{N-1}$ the DFT and inverse DFT are defined as

$$G_\ell = \sum_{j=0}^{N-1} e^{-i\frac{2\pi}{N}\ell j}\, g_j, \quad \ell = 0, \ldots, N-1 \tag{C.54}$$

$$g_j = \frac{1}{N} \sum_{k=0}^{N-1} e^{i\frac{2\pi}{N}\ell j}\, G_\ell, \quad j = 0, \ldots, N-1 \tag{C.55}$$

The DFT and inverse DFT can be efficiently evaluated by using the FFT and IFFT algorithm with the notation,

$$\mathbf{G}_N = \text{FFT}(\mathbf{g}_N) \tag{C.56}$$

$$\mathbf{g}_N = \text{IFFT}(\mathbf{G}_N) \tag{C.57}$$

European Vanilla Call Option

Denote $s = \ln S_T$ and $k = \ln K$. The price of this call option is then given by

$$\Pi(k) = e^{-rT} \int_k^\infty (e^s - e^k) f(s)\, ds \tag{C.58}$$

where $f(s)$ is the risk-neutral density of $\ln S_T$.

doi:10.6342/NTU202101125

The function Π is not square-integrable because $\Pi(k)$ converges to S_0 for $k \to -\infty$. Hence, we consider a modified function:

$$\widetilde{\Pi}(k) = e^{\alpha k}\,\Pi(k) \tag{C.59}$$

which is square-integrable for a suitable $\alpha > 0$. The choice of α may depend on the model for S_t.

Taking the Fourier transform of the modified call function gives

$$\begin{aligned}
\Upsilon(u) &= \int_{-\infty}^{\infty} e^{iuk}\,\widetilde{\Pi}(k)\,dk = \int_{-\infty}^{\infty} e^{(iu+\alpha)k}\,\Pi(k)\,dk && \text{(C.60)}\\
&= \int_{-\infty}^{\infty}\int_{k}^{\infty} e^{(iu+\alpha)k}e^{-rT}(e^s - e^k)f(s)\,ds\,dk && \text{(C.61)}\\
&= \int_{-\infty}^{\infty} e^{-rT} f(s) \int_{-\infty}^{s} \left(e^{s+\alpha k} - e^{(1+\alpha)k}\right) e^{iuk}\,dk\,ds && \text{(C.62)}\\
&= \int_{-\infty}^{\infty} e^{-rT} f(s) \left(\frac{e^{(\alpha+1+iu)s}}{\alpha+iu} - \frac{e^{(\alpha+1+iu)s}}{\alpha+1+iu}\right) ds && \text{(C.63)}\\
&= \frac{e^{-rT}\,\psi\big(u - i(\alpha+1)\big)}{\alpha^2+\alpha-u^2+iu(2\alpha+1)} && \text{(C.64)}
\end{aligned}$$

where $\psi(u) = \hat{f}(u) = \int_{-\infty}^{\infty} e^{ius} f(s)\,ds$ is the Fourier transform of $f(s)$.

Finally, to get the call price function $\Pi(k)$, perform the Fourier inversion, i.e.

$$\Pi(k) = e^{-\alpha k}\,\widetilde{\Pi}(k) = \frac{e^{-\alpha k}}{2\pi}\int_{-\infty}^{\infty} e^{-iuk}\,\Upsilon(u)\,du = \frac{e^{-\alpha k}}{\pi}\int_{-\infty}^{\infty} e^{-iuk}\,\Upsilon(u)\,du \tag{C.65}$$

The last equality holds because $\Pi(k)$ is real, which implies that the function $\Upsilon(u)$ is odd in its imaginary part and even in its real part.

doi:10.6342/NTU202101125

Approximate this integral with interval width Δu to get

$$\Pi(k_\ell) \approx \Delta u \, \frac{e^{-\alpha k_\ell}}{\pi} \sum_{j=0}^{N-1} e^{-iu_j k_\ell} \, \Upsilon(u_j) \, \omega_j \tag{C.66}$$

where $u_j = j\Delta u$, $j = 0, 1, \ldots, N-1$, $\Delta u > 0$ is the distance between the points of the integration grid, and ω_j is the weight that depends on the type of quadrature.

Consider an equidistant spacing of the log-strikes around the log spot price s_0:

$$k_\ell = -\frac{1}{2} N\Delta k + \ell\Delta k + s_0, \qquad \ell = 0, 1, \cdots, N-1 \tag{C.67}$$

where $\Delta k > 0$ denotes the distance between the log strikes.

Δu and Δk are chosen such that they satisfy the so called Nyquist criterion:

$$\Delta k \Delta u = \frac{2\pi}{N} \tag{C.68}$$

This constraint leads, however, to the following trade-off: the parameter N controls the computation time and thus is often determined by the computational setup. Hence the right hand side may be regarded as given or fixed. One would like to choose a small Δk in order to get many prices for strikes near the spot price. But the constraint implies then a big Δu giving a coarse grid for integration. So we face a trade-off between accuracy and the number of interesting strikes.

doi:10.6342/NTU202101125

The above numerical approximation can be expressed as

$$\Pi(k_\ell) \approx \Delta u \, \frac{e^{-\alpha k_\ell}}{\pi} \sum_{j=0}^{N-1} e^{-i(j\Delta u)\left(\ell\Delta k - \frac{N}{2}\Delta k + s_0\right)} \, \Upsilon(u_j)\, \omega_j \tag{C.69}$$

$$= \Delta u \, \frac{e^{-\alpha k_\ell}}{\pi} \sum_{j=0}^{N-1} e^{-i\frac{2\pi}{N}\ell j} \, e^{i\left(\frac{N}{2}\Delta k - s_0\right)u_j} \, \Upsilon(u_j)\, \omega_j \tag{C.70}$$

The FFT can be applied to

$$\mathbf{\Pi} = \mathbf{C} \odot \mathrm{FFT}(\mathbf{\Psi}) \tag{C.71}$$

where

$$\mathbf{\Pi} = [\Pi(k_0), \ldots, \Pi(k_{N-1})] \tag{C.72}$$

$$\mathbf{C} = [C_0, \ldots, C_{N-1}] \tag{C.73}$$

$$C_\ell = \Delta u \, \frac{e^{-\alpha k_\ell}}{\pi} \tag{C.74}$$

$$\mathbf{\Psi} = [\Psi_0, \ldots, \Psi_{N-1}] \tag{C.75}$$

$$\Psi_j = e^{i\left(\frac{N}{2}\Delta k - s_0\right)u_j} \, \Upsilon(u_j)\, \omega_j \tag{C.76}$$

C.5 Two-Dimensional FFT

Continuous Fourier Transform (CFT)

The Fourier transform of $f(x_1, x_2)$ is defined as follows:

$$\mathcal{F}[f(x_1,x_2)](u_1,u_2) := \hat{f}(u_1,u_2) = \int_{-\infty}^{\infty}\int_{-\infty}^{\infty} e^{-i(u_1x_1+u_2x_2)} \, f(x_1,x_2)\, dx_1\, dx_2 \tag{C.77}$$

doi:10.6342/NTU202101125

and the corresponding inversion formula is given by

$$f(x_1, x_2) = \frac{1}{4\pi^2} \int_{-\infty}^{\infty} \int_{-\infty}^{\infty} e^{i(u_1 x_1 + u_2 x_2)} \hat{f}(u_1, u_2)\, du_1\, du_2 \tag{C.78}$$

The characteristic function of a continuous univariate random variable, with its probability density function f, is defined as a Fourier transform of its PDF,

$$\hat{f}(u_1, u_2) := \psi(u_1, u_2) \tag{C.79}$$

Discrete Fourier Transform (DFT)

For complex numbers $g_0, \ldots, g_{N-1}$ the DFT and inverse DFT are defined as

$$G_{p,q} = \sum_{j=0}^{M-1} \sum_{k=0}^{N-1} e^{-i\frac{2\pi}{M}jp} e^{-i\frac{2\pi}{N}kq} g_{j,k}, \quad p = 0, \ldots, M-1, \quad q = 0, \ldots, N-1 \tag{C.80}$$

$$g_{j,k} = \frac{1}{M} \sum_{p=0}^{M-1} \frac{1}{N} \sum_{q=0}^{N-1} e^{i\frac{2\pi}{M}jp} e^{i\frac{2\pi}{N}kq} G_{p,q}, \quad j = 0, \ldots, M-1, \quad k = 0, \ldots, N-1 \tag{C.81}$$

The DFT and inverse DFT can be efficiently evaluated by using the FFT and IFFT algorithm with the notation,

$$\mathbf{G}_{M\times N} = \text{FFT2}(\mathbf{g}_{M\times N}) \tag{C.82}$$

$$\mathbf{g}_{M\times N} = \text{IFFT2}(\mathbf{G}_{M\times N}) \tag{C.83}$$

doi:10.6342/NTU202101125